

Article

International Migration Projections across skill levels in the Shared Socioeconomic Pathways

Soheil Shayegh^{1,*}, Johannes Emmerling¹ and Massimo Tavoni^{1,2}

¹ RFF-CMCC European Institute on Economics and the Environment (EIEE), Centro Euro-Mediterraneo sui Cambiamenti Climatici, Italy

² Department of Management and Economics, Politecnico di Milano, Italy

* Correspondence: soheil.shayegh@eiee.org

Abstract: International migration is closely tied to demographic, socioeconomic, and environmental factors and their interaction with migration policies. Using a combination of a gravity econometric model and an overlapping generations model, we estimate the probability of bilateral migration among 160 countries in the period of 1960 to 2000 and use these findings to project international migration flows and their implication for income inequality within and between countries in the 21st century under five shared socioeconomic pathways (SSPs). Our results show that international migration not only increases the welfare in developing countries, but also closes the inequality gap within and between low-skilled and high-skilled labor in these countries. In most developed countries on the contrary, international migration increases the inequality gap and slightly reduces output. These changes are not uniform and vary significantly across countries depending on their population growth and human capital development trajectories. Overall, while migration is strongly affected by inequality between developed and developing countries, it has an ambiguous impact on inequality within and between countries.

Keywords: Migration; Shared Socioeconomic Pathways; Inequality; Labor; Demographics; Human capital

1. Introduction

International migration fosters inter-cultural exchanges and provides opportunities for people to relocate in search of better living conditions [1]. Despite a relatively stable trend over the last part of the twentieth century [2], the United Nations (UN) has estimated that between 2000 and 2017 the stock of international migrants increased from 173 to 258 million people, accounting for about 3.4 percent of global population [3]. The increase in international migration is expected to continue due to rise in socioeconomic inequality and climate change among other factors [4,5]. In this paper we first examine whether and to what extent demographic change and income inequality have shaped historical international migration flows. We use our findings to show (a) how assumptions about future human capital accumulation and climate change will impact the projections of international migration flows, and (b) how the projections of international migration flows will change wealth distribution and income inequality within and between countries and skill groups by the end of the century.

Global studies of migration have been largely divided in two camps. One group of literature, have used statistical models to identify the key determinants and drivers of international migration and use these models to project the future trends [6,7]. We follow the leading literature in this category to develop a broad gravity model of bilateral migration flows among 160 countries in the period of 1960-2000 which helps us identify the key drivers of international migration. However, relying solely on econometric models for projecting the future outcomes, requires strong limiting assumptions about migration trends. For example, the UN projections of international migration have been largely based on a simple assumption that levels of net migration will be kept constant at their current levels until 2045-2050 and then will gradually decline to 50 per cent of the projected level of 2045-2050 by 2100 [8,9].

In order to improve the insights from statistical methods, another group of literature have tried to account for the interdependencies in future distributions of income, population and migration by developing structural models of economic growth [10,11]. These models provide an underlying explanation for migration mechanism that can be used to assess future migration projections under different socioeconomic scenarios [12,13]. In a similar fashion, here we develop a structural model to project future migration flows under five distinct shared socioeconomic pathways (SSP) scenarios [14]. This model allows us to observe the evolution of migration in the broader context of socioeconomic changes in the future and to examine the interaction between migration, demography, human capital, income inequality, and economic growth within a unified framework [12,15]. Therefore, the first contribution of our paper is to develop a structural model to show how underlying human capital accumulation trends within the SSP scenarios will shape the international migration patterns throughout the 21st century from the perspective of both sending and receiving countries.

The broader impact of migration on economic development and inequality has been long debated in the literature. While some previous studies show a negative impact of migration on the wages in receiving regions [16], they have shown that this impact is not homogeneous across skill levels. Immigration is shown to have a negative impact on the wages of low-skilled labor and a positive impact on the wages of high-skilled labor [17,18]. Other studies not only rule out the negative impact of immigration on the wages of native labor in receiving regions [19], but also show a positive increase in GDP of the receiving countries [20]. However, except few global studies [10,12], most of the literature in this field has been based on historical data from specific countries or regions. Hence, the second contribution of our paper is to identify the impact of international migration on income inequality and social welfare in sending and receiving countries across the SSP scenarios.

Finally, in addition to socioeconomic factors, environmental parameters can play a significant role in shaping migration trends. Recent studies on the impact of climate change on demographic change and population dynamics have highlighted important mechanisms through which climate change alters human capital accumulation that may trigger international migration as an adaptation response to extreme events [21–24]. These studies are mainly focused on the historical trend of migration and try to demonstrate a positive and statistically significant relationship between environmental factors (e.g., temperature and precipitation), and international migration [25–27]. While some studies find no evidence of the impact of climate change and natural hazards on international migration [28], other studies have highlighted the indirect effects of environmental factors on migration through changing wages [29] especially in agricultural economies [30]. Our statistical analysis demonstrates no evidence of direct impact of temperature rise on international migration flows. Nevertheless we include an explicit form of climate damage function in our structural economic model to account for future economic losses due to climate change and their impact on migration flows. In this manner, our paper is close to some of the most recent works on the intersection of international migration, inequality, and climate change [15,31,32]. It is worth mentioning that the emphasis of our model is on the long-term gradual movement of people within 20-year time periods and therefore, it does not account for the impacts of natural disasters and climate shocks on migration flows (i.e., crisis-induced migration [33]). We integrate representative concentration pathways (RCP) into our SSP scenario framework that allows us to consider a full spectrum of socioeconomic and climate factors concurrently. The third contribution of our paper is therefore, in its ability to combine not only statistical and structural models but also SSP and RCP scenarios to develop migration projections that can be interpreted within the future environmental and socioeconomic context.

2. The SSP-RCP Scenario Framework

Figure 1 shows the outline and the components of our modeling framework.

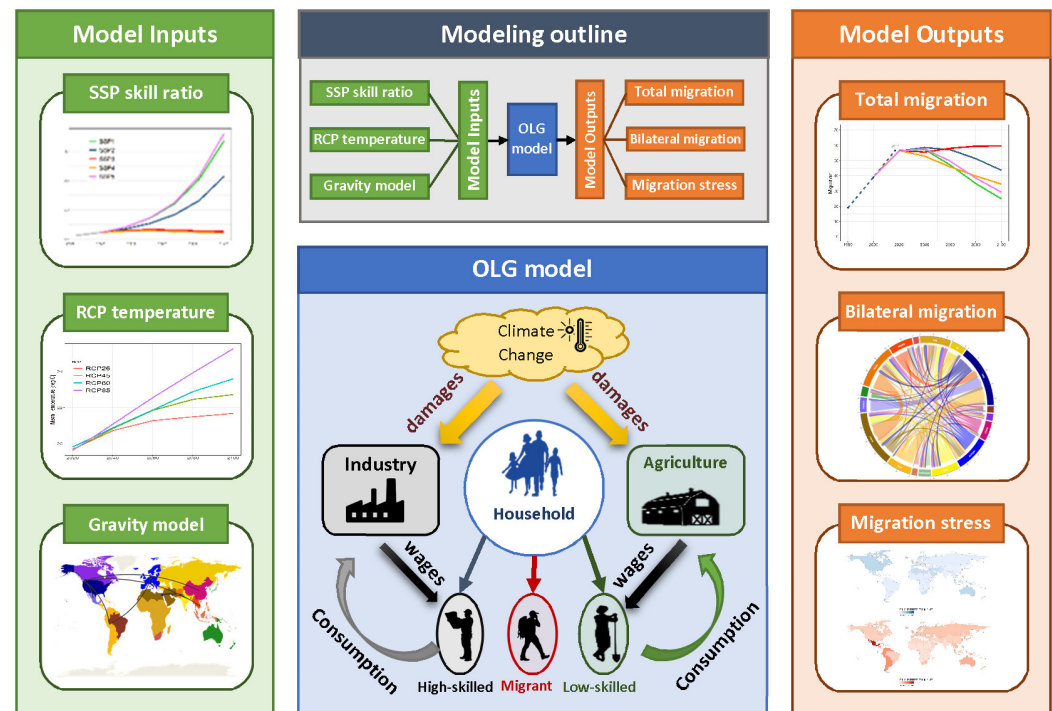


Figure 1. Modeling outline and its components. We use SSP database to generate projections of skill ratio. RCP scenarios provide temperature projections. The historical bilateral migration data are used to generate a gravity model of migration. The OLG model is calibrated with these inputs and generates total migration flows (figure 3), bilateral migration flows for each SSP scenario (figure 4), and migration stress maps.

The first input to our model is the SSP projections of human capital development for each country. This is quantified in our model as the skill ratio (e.g., the ratio of high-skilled adult population to low-skilled adult population) across SSP scenarios. Each SSP scenario comes with a unique trajectory of key socioeconomic indicators (see figure A2 in Appendix based on data from [14,34,35]). Under each SSP scenario, countries experience different economic growth rate and human capital accumulation trajectories [36]. As a result, socioeconomic conditions under each SSP may act as pull or push factors that will drive international migration flows in a non-uniform and heterogeneous way across the world [37]. The underlying narratives of SSP scenarios is presented in section Appendix.A.

In addition to the SSP projections of human capital accumulation, we integrate explicit assumptions about the future climate change in our model by including two RCP projections of country-specific temperatures. We report the main results of our model under RCP6.0 (*baseline case*) where global temperature will increase by about 3° C above pre-industrial levels by the end of the century [38]. The results associated with a lower climate change scenario of RCP2.6 are reported in section Appendix.D.3.

Finally, we develop a gravity model of historical bilateral migration data for 160 countries to find the key drivers of international migration. We find that the probability of future migration (i.e., percentage of migrants to the total population) depends on the current population, income inequality, and the distance between the sending and receiving countries. We use the coefficient of the gravity model to project the future migration trends within an overlapping generations (OLG) model of population dynamics. At the heart of our approach is an OLG model of population dynamic that is based on the SSP-RCP scenario projections and the results of the gravity model of bilateral migration probabilities. We aggregate the country-level results of the OLG model projections and present them at the regional level by dividing the world into 17 regions so that each region includes

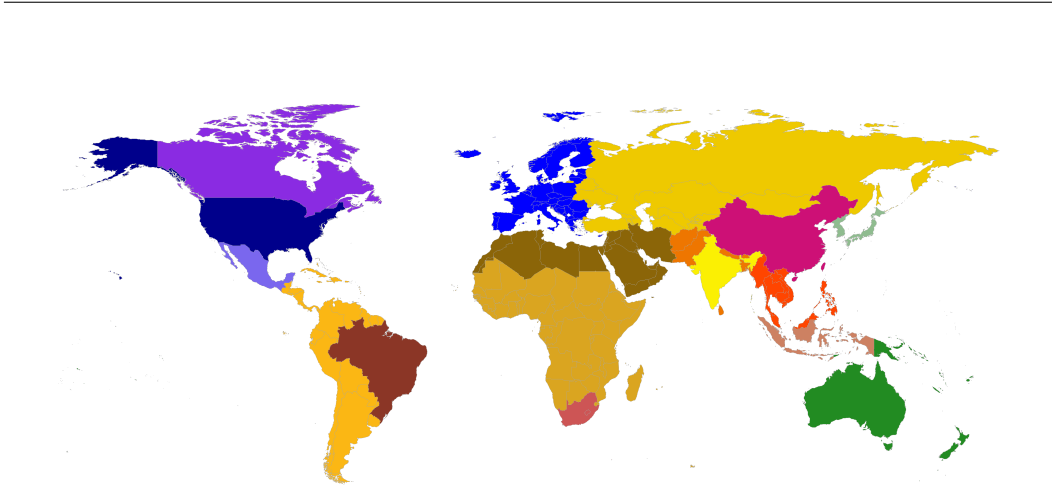


Figure 2. Seventeen geographical regions used for calculating global migration flows.

Table 1. Seventeen geographical regions used for calculating global migration flows along with the cover code used figures 2 and 4.

Region	Abbreviation	Color
Canada	CAN	
Japan-Korea	JPN	
Oceania	OCE	
Indonesia	IDN	
South Africa	ZAF	
Brazil	BRA	
Mexico	MEX	
China	CHN	
India	IND	
Non-EU Eastern European	TEC	
Sub Saharan Africa	SSA	
Latin America-Caribbean	LAC	
South Asia	SAS	
South East Asia	SEA	
Middle East-North Africa	MEA	
Europe	EUR	
USA	USA	

countries with similar socioeconomic status and geographical proximity (see figure 2 and table 1 for the definition of the regions).

3. Econometric Model

The skill dependent phenomenon of migration has been widely observed, and notably a skill-bias has been frequently found or discussed in migration patterns [39]. In order to calibrate the bilateral migration probabilities in our model, we use data on population and educational attainment [36], which also includes projections until 2100 for all the SSP scenarios. Moreover, we use historical data on GDP, income inequality, and population from the IMF’s World Economic Outlook [40,41]. Historical bilateral migration flow data is obtained from decadal data on country by country migration stocks [42]. Based on the country level data and similar to empirical studies on the determinants of migration, we estimate a gravity model equation of migration across countries. In particular, we estimate the following equation

$$\frac{M_{ij,t+1}^k}{L_{i,t+1}^k} = \theta_1^k \log(L_{i,t}^k) + \theta_2^k \log(L_{j,t}^k) + \theta_3^k \log\left(\frac{GDPPC_{j,t}^k}{GDPPC_{i,t}^k}\right) + \theta_4^k \log(d_{ij}) + \eta_i + \delta_j + \varepsilon_{ij}(1)$$

That is, at every time period t we estimate the probability of migration of adults of skill level k from sending country i to receiving country j at the next time period $t + 1$. This probability is calculated as the future flow of migrants ($M_{ij,t+1}^k$) per total adult population of the sending country ($L_{i,t+1}^k$). As in our economic model, the migration probability is a function of the current adult population in origin ($L_{i,t}^k$) and in destination ($L_{j,t}^k$), the wage ratio of receiving to sending country, and the distance between both countries (d_{ij}). We use per capita output of adult groups of skill level k measured in USD-PPP of 2005 ($GDPPC_{j,t}^k / GDPPC_{i,t}^k$) as a proxy for the wage ratio of receiving to sending country. We compute it by dividing the adult population into high-skilled and low-skilled groups based on education attainment records. Using the historical Gini index data for each country, we compute the wage for each skill group by matching the Gini index and per-capita GDP (two equations and two unknown wages). The distance is taken as the shortest distance between the borders of each two countries. Note that since we need to implement the formula in the analytical model, we use the simple linear probability model (LPM) to estimate this equation, and include both origin (η_i) and destination (δ_j) fixed effects to account for country-specific idiosyncratic drivers of migration.

Alternatively, we can estimate equation 1 using the Pseudo Poisson Maximum Likelihood (PPML) estimator of [43] to account for zeros in the observed migration probabilities and heteroscedasticity (see section Appendix.D.1 for the discussion about the suitability of the PPML model in projecting future migration probabilities). However, we find that in terms of the relevant drivers, the estimates coefficients are rather similar.

We estimate equation (1) using different specifications. For the model calibration, our central estimation is a standard OLS estimation of the migration probability, so that the correlation with GDP, population, and distance is taken into account in the model. We also include country-specific autonomous terms. The results of the econometric model are presented in section Appendix.B.

4. Overlapping Generations Model

We develop a structural model of population dynamic and economic growth to project the future global population growth and international migration flows. In this model, we account for two groups of high-skilled and low-skilled labor who work in agricultural and non-agricultural sectors respectively. Individuals live through two periods: childhood, and adulthood. The decision about the number of children (population growth) and their skill level (human capital) is made by parents through the optimization of the parental utility function. Parents are altruistic which means their utility increases not only through consumption of goods but also through expected well-being of their children. There is a quantity-quality trade-off in raising children in a sense that high-skilled children with potentially higher income in their adulthood require more parental investment in their childhood. We calibrate this model to reflect the projection of human capital development for each country under the five SSP scenarios. In each period, the projections of climate conditions for the next period are obtained from the RCP projections and used for calculating climate-induced damages to each economic sector. In addition, the probability of bilateral migration of high-skilled and low-skilled adults is endogenous and calculated based on the results of the gravity model in equation (1) in section 3. We modify the migration probability specified in this equation to use it in our OLG model:

$$\beta_{ij,t+1}^k = \theta_{ij}^k + \theta_1^k \log(L_{i,t}^k) + \theta_2^k \log(L_{j,t}^k) + \theta_3^k \log\left(\frac{w_{j,t}^k}{w_{i,t}^k}\right) + \theta_4^k \log(d_{ij}) + \eta_i + \delta_j, \quad (2)$$

where migration probability ($\beta_{ij,t+1}^k$) indicate the portion of individuals with skill level k from country i that will migrate to country j at the next time step $t + 1$. This probability is a function of the current population of adults with the same skill level k in the sending country ($L_{i,t}^k$) and receiving country ($L_{j,t}^k$), the current ratio of wages between the same

type of labor in two countries ($\frac{w_{j,t}^k}{w_{i,t}^k}$), the distance between the two countries (d_{ij}), and the sending and receiving countries' fixed effects (η_i and δ_j). The parameter θ_{ij}^k is the migration residual between the two countries calculated from fitting the probability equation to historical migration data from 1980 to 2000.¹ The detailed description of the OLG model, its calibration, and the solution methodology are provided in section Appendix.C.

5. Projections of migration and demographic outcomes

The output of the OLG model is a set of future migration flows across the SSP scenarios as shown in figure 1. As we outlined in section 2, each SSP revolves around a unique narrative about future socioeconomic and technological developments. For example, SSP1 and SSP5 have very different assumptions about fossil-fuel consumption and related emissions but they have very similar population growth and human capital accumulation trajectories [36]. As a result, the projections of total migration flows overlap in these two scenarios.² Although the SSP5 narrative assumes higher levels of international migration compared to SSP1, our baseline OLG model (using only SSP skill ratio as an input) is not able to capture such differences without further assumptions about migration policies. Therefore, in section Appendix.D.2 we have introduced a modified version of equation (A1) with an exogenous SSP-specific migration policy parameter that will allow the model to distinguish between the migration dynamics in SSP1 and SSP5 scenarios.

Another important driver of migration is the income inequality between receiving and sending regions represented by the wage differences between countries in equation (A1). The impact of income inequality on migration flows can be observed by comparing SSP2 and SSP4 scenarios. These two scenarios have similar global population growth but very different human capital accumulation trajectories [36]. The SSP2 scenario projects a moderate growth in human capital accumulation specially in developing regions. The SSP4 scenario on the other hand, projects a halt or even a decline in human capital growth for most regions. As a result, SSP4 experiences higher inequality and much larger migration flows. Throughout our analysis we refer to the difference between the results of these two scenarios as *inequality effect*.

Finally, climate change induced damages in different sectors can potentially create new mechanisms for labor movement within and between countries. Here we present the results of our analysis for the case of RCP6.0 temperature trajectories (i.e., the *baseline case*). The results of a case with limited climate change (RCP2.6) are presented in the in section Appendix.?? and show a very similar pattern to the results of the *baseline case*. Panel (a) in figure 3 shows the total migration flows for every 20 years under the five SSP scenarios. In the SSP1, SSP2, and SSP5 scenarios, the migration flow peaks around 2060, and declines afterwards. In the SSP3 and SSP4 scenarios however, the migration flow rapidly increases until it reaches its maximum by the end of the century. Comparing the results under SSP2 and SSP4 reveals that *Inequality effect* changes both the size and shape of the migration flows. We can further disintegrate the migration flows by the skill level of migrants. Panel (b) and panel (c) in figure 3 show the projections of global flow of high-skilled labor and low-skilled labor respectively. In the SSP1, SSP2, and SSP5 scenarios, high-skilled migration accounts for the majority of total migration flows while in SSP3 and SSP4 it accounts for about half of total migration.

Figure 4 shows the bilateral flow of migrants across 17 aggregated regions in the period of 2080-2100 for the five SSP scenarios and compares it with historical bilateral

¹ In a modified version of equation (A1) in section Appendix.D.2, we have implemented an exogenous policy parameter to this equation to account for migration policy variations across SSP scenarios.

² As our gravity model shows and as the comparison between the results of our *baseline case* here and the RCP2.6 case in in section Appendix.D.3 further suggests, we can safely assume that gradual climate change (and not climate shocks and catastrophes) does not have a direct impact on long-term migration trajectories.

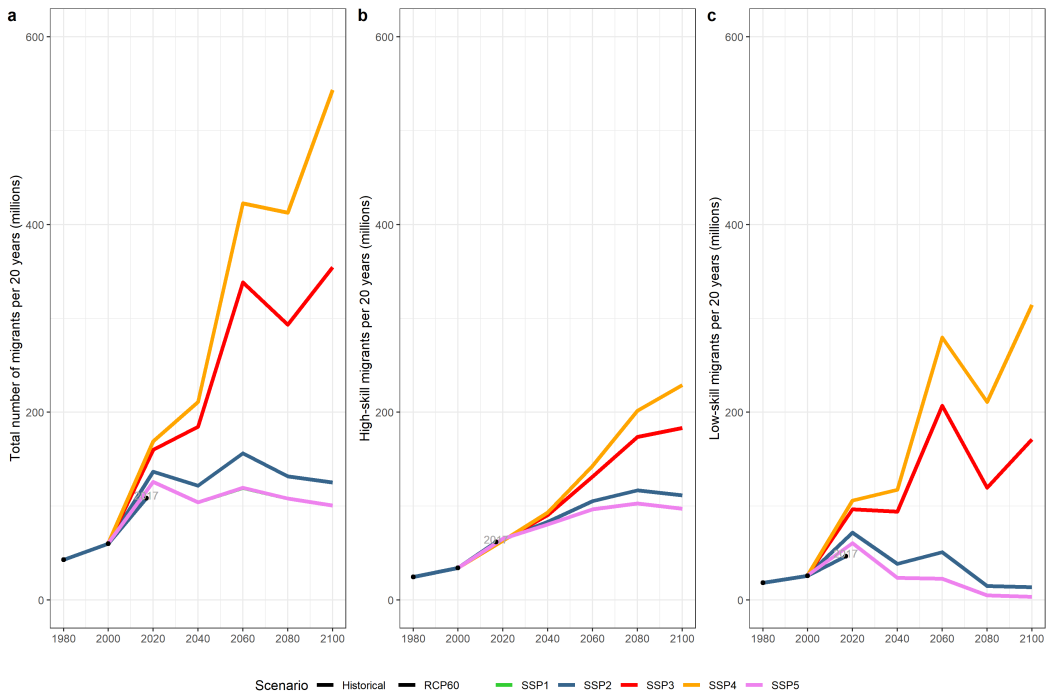


Figure 3. Historical and projections of twenty-year global migration flows across the SP scenarios (a) Total global migration. (b) High-skilled global migration. (c) Low-skilled global migration. The global share of skilled migrants is around 57% of total migrants compatible with existing estimates of the skill-bias of migration. The focus on periods of 20 years reflects the duration of a generation in our OLG model. We have aggregated historical migration data that are provided for each decade to obtain the 20-year historical flows. We have excluded historical data for the 2000-2010 period due to their inconsistency.

flows from the 1980-2000 period.³ Regardless of underlying SSP assumptions, there are few notable migration trends in all the SSP scenarios (e.g., Europe emerges as a main destination while India becomes a major sending region). The SSP1 and SSP5 graphs in figure 4 show a very similar composition of bilateral flows. In contrast, comparing the SSP2 and SSP4 graphs paints a different picture: while the historical bilateral migration flows are dominated by few main trends (e.g., Mexico and Latin America to the U.S.), the medium range growth rate of economy and education under the SSP2 scenario leads to a more homogeneous flow of migrants between developing and developed regions in the future. In the inequality-driven world of the SSP4 scenario however, migration trends are still dominated by the South-to-North or Developing-to-Developed flows, notably from India and Sub-Saharan Africa to Europe.

Inequality in skill and education not only drives migration but also evolves as a result of migration and the subsequent redistribution of wealth and labor in sending and receiving countries. In our dynamic model of population dynamics and migration, income disparity between the two types of labor and the heterogeneity of climate change damages create incentive for parents to have specific number and type of children in each period. This in turn, changes the migration probabilities and induces some movement of labor among countries. Once all bilateral migrations are completed, labor markets will be cleared, new wages will be realized, and income inequality within and between regions will evolve accordingly. Figure 5 shows a snapshot of the inequality measures for the year 2080 across the SSP scenarios for the two cases: with migration, and without migration. In the case without migration we assume zero bilateral migration and therefore the inequality indicators are driven only by demographic change and labor allocation within each country. In order to quantitatively compare the results, here we focus on the SSP2 scenario as a middle of the road scenario.

Panel (a) in figure 5 shows the relative wages of low-skilled labor in each region compared to global average. In developed regions (depicted in darker colors, starting from the U.S. at the top and moving clockwise), the wages of low-skilled labor are much higher than the average in the case without migration. For example, in Canada (CAN) the wages of low-skilled labor is about 3.8 times the global average in the case without migration but when migration is allowed, it is much lower at about 0.2 times the global average. Meanwhile the wages of low-skilled labor in developing countries improve to close the global inequality gap for the low-skilled labor when migration is allowed. For example, the wages of low-skilled labor in South East Asia (SEA) increase from 0.03 times the global average in the case without migration to about 0.2 times the global average in the case with migration. Overall, migration reduces global inequality among low-skilled labor across the SSP scenarios, while the rate of reduction is lower in SSP3 and SSP4.

Panel (b) in figure 5 shows the relative wages of high-skilled labor in each region compared to global average. The overall change in relative wages of high-skilled labor seems to follow a similar pattern but at lower rate. For example, in Canada, the wages of high-skilled labor are about 3.3 times the global average without migration and they fall slightly below this level when migration is allowed (3.1 times the global average). On the other hand, wages of high-skilled labor in developing countries slightly increase under most of the SSP scenarios. For example, the wages of high-skilled labor in South Africa (ZAF) stay around 0.6 times the global average with or without migration. Overall, global inequality among high-skilled labor is slightly improved by migration.

In order to compare the inequality within each region we calculate the wage ratio of high-skilled labor to low-skilled labor in panel (c) in figure 5. In developed regions, the inequality between high-skilled and low-skilled labor is increasing with migration. This increase is even higher in inequality-driven SSP4. For example, in the U.S. (USA) the wage ratio of high-skilled to low-skilled labor increases from 10.6 in the case without migration

³ These circular plots show the total number of migrants on a circle with arrows from and to each of the 17 macro regions we aggregate country level data to. The numerical scale on the circles indicates the number of total migrants in hundred thousands.

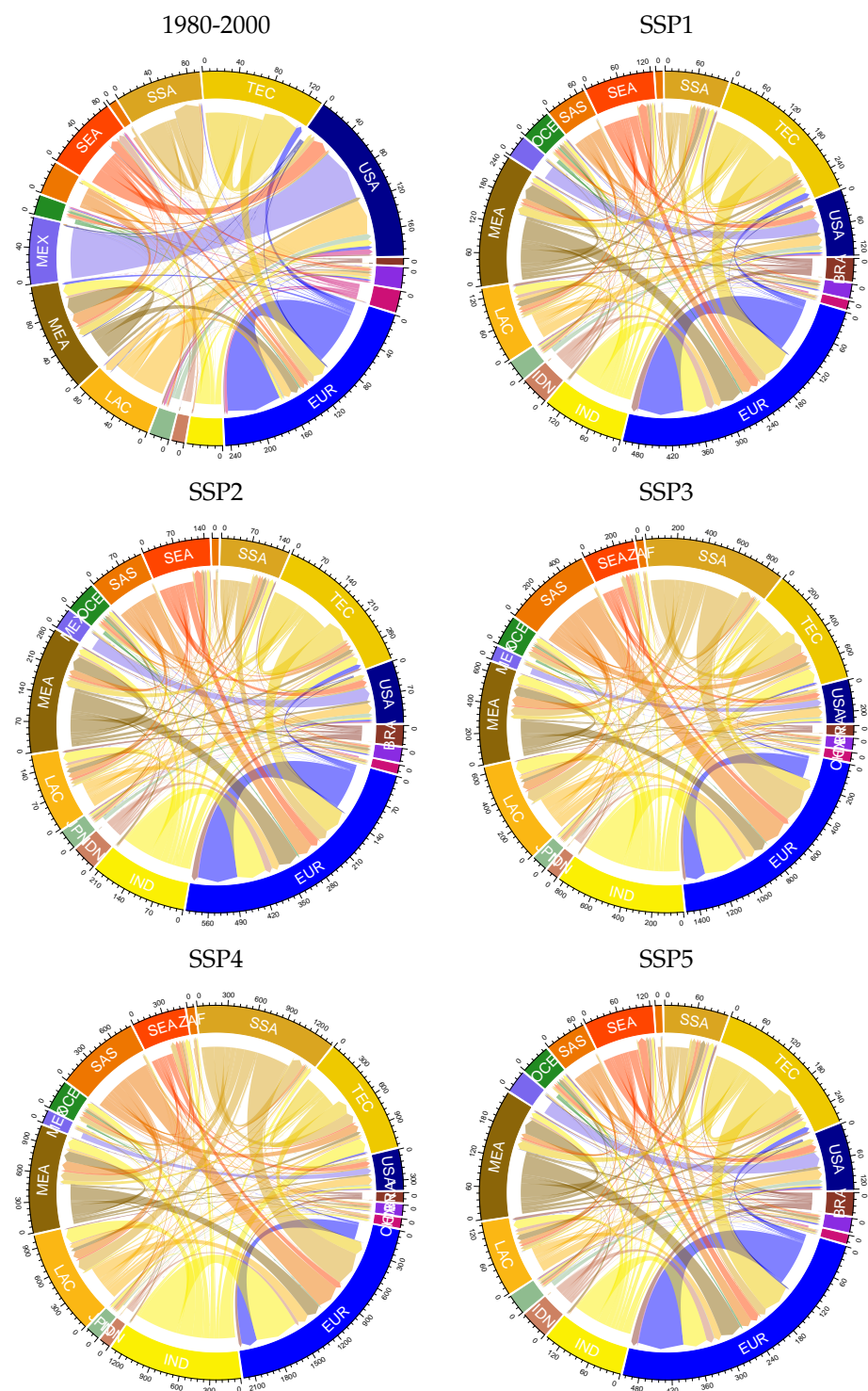


Figure 4. Regional bilateral migration flows, in 2080-2100 period, annually in 100 thousands in the SSP scenarios

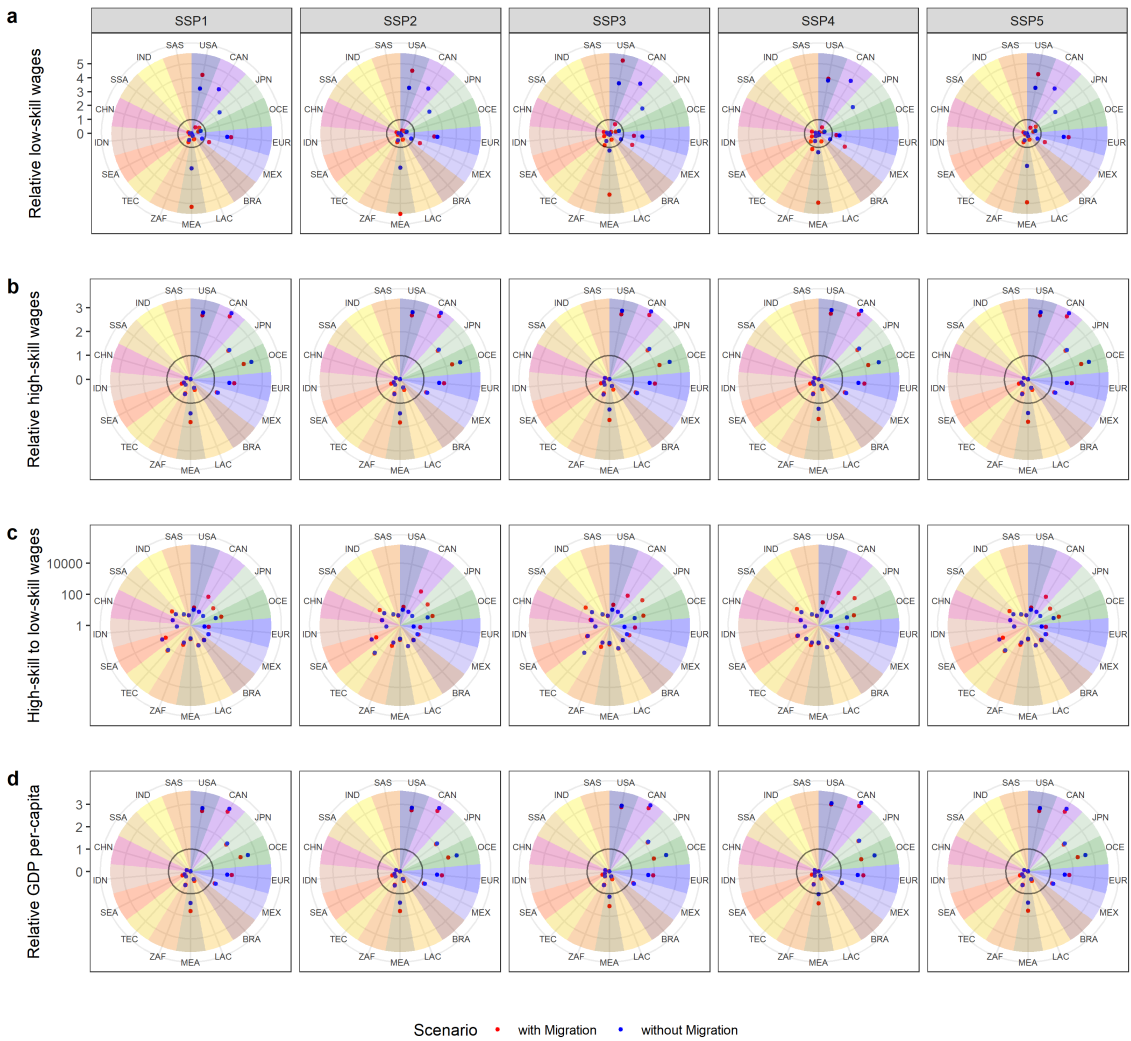


Figure 5. Income inequality across the regions and the SSP scenarios in 2080 with and without Migration. (a) Relative wages of low-skilled labor to global average. (b) Relative wages of high-skilled labor to global average. (c) Relative wages of high-skilled labor to low-skilled labor in logarithmic scale. (d) Relative GDP per capita to global average. Dark circle in the middle in rows (a), (b), and (d) identifies the global average. The regions have been ordered based on their per capita GDP in year 2000, starting from the USA with the highest and moving clockwise to the Sub-Saharan Africa (SSA) with the lowest.

to 16 in the case with migration. At the same time, income inequality in developing regions slightly declines or remains unchanged. For example, in Latin America (LAC) the wage ratio of high-skilled to low-skilled labor decreases from 28 in the case without migration to 27 in the case with migration. This is in line with the studies that show a positive impact of migration in reducing inequality specially in sending regions [44]. Overall, we observe that while migration reduces global inequality between regions, specially for low-skilled labor, it increases inequality within developed regions. This is in part because of the reduction in the wages of low-skilled labor in receiving regions due to immigration.

Finally, panel (d) in figure 5 demonstrates global inequality in terms of output per capita. The results are to some degree similar to the pattern we observed in panel (b) for the relative wages of high-skilled labor. While migration slightly decreases the relative GDP per capita in developed regions, it increases the relative GDP per capita in developing regions.

6. Discussion and conclusions

In this paper we developed a modeling framework for projecting bilateral international migration flows throughout the 21st century across the five SSP scenarios. We used historical bilateral migration data for 160 countries in a gravity model that takes into account natural drivers (e.g., distance) and socioeconomic drivers (e.g., wage disparity between receiving and sending regions). We applied our empirical findings to an overlapping generations model [31,32] to generate projections of population growth, demographic change, and migration flows for each country. Our findings can be summarized in four categories.

First, we find that the structure and direction of migration is predominantly defined by underlying socioeconomic assumptions including inequality within and between countries and skill groups. For example, while SSP2 and SSP4 share similar population growth trajectories, due to their different human capital development trajectories (e.g., different skill ratios), the migration scale and pattern in these two scenarios greatly diverge.

Second, we show that international migration has a more clear impact on closing the inequality gap among low-skilled labor while its impact on closing the inequality gap among high-skilled labor is less obvious.

Third, we find that as a result of international migration, the inequality gap between high-skilled and low-skilled labor increases significantly in developed countries while it reduces slightly in developing countries. In other words, while developing countries experience higher inequality at the beginning, migration will exert a greater pressure on equality in receiving countries that are predominantly developed.

Finally, comparing migration flows over time and across the SSP scenarios, we observe that while some major developed regions like Europe will gain positive economic benefits from migration at the cost of increasing inequality, other developed countries will experience both an economic loss and an increase in inequality as a result of migration. On the other hand, most developing regions gain economic benefits from migration and manage to close the inequality gap within and between their low-skilled and high-skilled labor force.

Author Contributions: Conceptualization, S.S., J.E., and M.T.; methodology, S.S. and J.E.; validation, S.S. and J.E.; formal analysis, S.S. and J.E.; investigation, S.S. and J.E.; resources, S.S. and J.E.; data curation, J.E.; writing—original draft preparation, S.S. and J.E.; writing—review and editing, S.S., J.E., and M.T.; visualization, S.S. and J.E.; supervision, M.T.; funding acquisition, J.E. All authors have read and agreed to the published version of the manuscript.

Funding: This research was funded by the European Union's Horizon 2020 research and innovation programme under grant agreements No 821124 - NAVIGATE - Next generation of AdVanced InteGrated Assessment modelling to support climaTE policy making.

Institutional Review Board Statement: Not applicable.

Informed Consent Statement: Not applicable.

Data Availability Statement: Data was obtained from the World Bank and are publicly available at <https://databank.worldbank.org/source/global-bilateral-migration>.

Conflicts of Interest: The authors declare no conflict of interest.

Appendix A. SSP narratives

SSP1 is the sustainability scenario with a medium level of migration where the world gradually moves toward low-emission technologies with higher rates of education and human capital accumulation. Investments in educational and health accelerate the demographic transition, and inequality is reduced both across and within countries. **SSP2** is the middle of the road scenario with a medium level of migration and moderate challenges to mitigation and adaptation. In this scenario, the world follows a business-as-usual development path. It experiences environmental degradation with a decline in intensity of resource and energy use. Global population grows moderately and levels off in the second half of the century. There will be slow improvements in income inequality and environmental challenges.

SSP3 represents a world filled with regional rivalry with a low level of migration and high challenges to mitigation and adaptation. In this world, nationalism and concerns about competitiveness and security provoke regional conflicts and a decline in investments in education and technological development. Slow economic development coupled with high population growth in developing countries exert large pressure on natural resources and environmental indicators.

SSP4 is the inequality scenario with medium levels of migration where economies are growing in different rates across the globe. The world will be divided between highly educated societies with access to high technologies and capital and resources and lower-income, poorly educated societies with low-tech economy.

SSP5 represents a world with a high level of migration where economic development is closely tied to high fossil-fueled consumption. Technological progress is rapid and human capital grows fast. Investments in health, education, and institutions increases as global population peaks and declines in the 21st century.

Appendix B. Econometric model: data and results

Table A1. Summary Statistics

Statistic	N	Mean	St. Dev.	Min	Max
population_origin	38,416	35.929	127.241	0.115	1,269.117
governance_origin	24,800	0.531	0.195	0.128	0.954
gdppc_origin	38,416	9,862.675	15,351.970	176.507	105,723.400
gini_origin	27,696	0.390	0.090	0.206	0.661
temperature_mean_origin	38,416	19.165	6.845	−1.313	28.878
adults_origin	38,416	23.126	83.544	0.062	891.457
adults_s_origin	38,416	11.515	43.661	0.005	545.809
adults_u_origin	38,416	11.611	44.958	0.013	417.970
I_u_origin	27,696	1,619.118	2,258.951	37.790	12,482.420
I_s_origin	27,696	14,930.430	18,537.480	427.439	115,032.800
migration_stock	50,338	6,920.799	99,573.170	0.000	9,367,910.000
distance	55,138	5,525.726	4,379.361	1.000	19,147.900
migration_flow	24,144	4,270.829	63,890.900	0.000	6,959,408.000
migration_probability	19,883	0.001	0.006	0.000	0.257
migration_probability_u	19,883	0.002	0.019	0.000	0.683
migration_probability_s	19,883	0.002	0.018	0.000	0.756
temp_change_origin	12,656	0.439	0.747	−0.914	2.619

Table A2. Migration Gravity Model estimation (OLS)

	Pooled	High-skilled	Low-skilled
$\log(L_i)$	-0.56*	0.17	0.47
	(0.26)	(0.27)	(0.34)
$\log(L_j)$	-0.23	-0.38	-0.38
	(0.26)	(0.28)	(0.34)
$\log\left(\frac{GDPPC_j}{GDPPC_i}\right)$	0.52***	0.17	0.41*
	(0.14)	(0.26)	(0.16)
$\log(d_{ij})$	-0.08***	-0.06***	-0.06***
	(0.01)	(0.02)	(0.02)
R ²	0.11	0.13	0.13
Adj. R ²	0.10	0.11	0.11
Num. obs.	25117	15629	15629

All estimations include origin and destination fixed effects.

Table A1 summarizes the data used for the gravity model estimation. The main data source is the historical population and education data based on [36]. Based on the education and age group data, we compute the adult population (15-70 years) according to different educational attainment, and the population of children (less than 15 years old). The GDP data is based on combining IMF-WEO historical data and the SSP projections from [41]. In order to compute the wage ratio and GDP per capita for each of the two skill-level groups, we combine the GDP data with inequality data based on income quintiles from the World Development Indicators.

Table A2 shows the estimation results for the whole population, and separated estimations for high-skilled and low-skilled adults. The results confirm a strong effect of relative wages between origin and destination region specially for low-skilled labor. Moreover, the population of origin country has a positive effect, with a higher coefficient for low-skilled migrants. The distance had a negative and robust impact on migration as expected.

Although we use the bilateral migration data from 1960 to 2000 in our econometric model, we only show the 1980-2000 data in the forthcoming graphs for the purpose of comparison with SSP projections throughout the paper. Furthermore, we use the 1980-2000 data to calibrate and match the migration probability calculated in the structural model in the next section with the 2000 migration data.

Appendix C. OLG Model Description

We develop a structural model of economic and demographic change based on an overlapping generation (OLG) framework [45,46]. The model includes two types of labor and a two-sector economy, and a large set of I countries $j = 1, \dots, I$. This simple nature of model enables us to derive closed form solutions that can be applied for the socioeconomic projections. One economic sector is agriculture (a) where only low-skilled labor (u) is employed [47,48]. The other sector is non-agriculture (b) that uses only high-skilled labor (s). We obtain the explicit form of the bilateral migration probabilities from the gravity model based on historical migration data. This model reflects the fact that migration decisions are based mainly on income considerations [49]. According to the results of our gravity model, the probability of an individual with skill level k at time $t + 1$ to migrate from country i to country j is a function of the population of people with the same skill level k in the sending and receiving countries at time t ($L_{i,t}^k$ and $L_{j,t}^k$, respectively), the ratio of wages between the same type of labor in two countries at time t ($\frac{w_{j,t}^k}{w_{i,t}^k}$), the distance

between the two countries (d_{ij}), and the sending and receiving countries fixed effects (η_i and δ_j):

$$\beta_{ij,t+1}^k = \theta_{ij}^k + \theta_1^k \log(L_{i,t}^k) + \theta_2^k \log(L_{j,t}^k) + \theta_3^k \log\left(\frac{w_{j,t}^k}{w_{i,t}^k}\right) + \theta_4^k \log(d_{ij}) + \eta_i + \delta_j, \quad (\text{A1})$$

where θ_{ij}^k is the migration residual between the two countries calculated from fitting the probability equation to historical migration data from 1980 to 2000.

Appendix C.1. Preferences

Adult's utility comes from their level of consumption and from the future wages of their children:

$$v(c_t, n_t^s, n_t^u) = (1 - \gamma) \ln(c_t) + \gamma [\ln(n_t^s \mathbf{E} w_{t+1}^s + n_t^u \mathbf{E} w_{t+1}^u)], \quad (\text{A2})$$

where n_t^k is the number of children of skill level k , c_t is consumption of a bundle of agricultural and non-agricultural goods, and $\mathbf{E} w_{t+1}^k$ is the expected wages of children with skill level k depending on where the children will earn their income. The utility from the expected wages of children in country i is therefore calculated as

$$\begin{aligned} \ln(n_t^s \mathbf{E} w_{t+1}^s + n_t^u \mathbf{E} w_{t+1}^u) = \\ \ln\left(n_t^s \sum_{j=1}^I \beta_{ij,t+1}^s w_{t+1}^{j,s} + n_t^u \sum_{j=1}^I \beta_{ij,t+1}^u w_{t+1}^{j,u}\right), \end{aligned} \quad (\text{A3})$$

For simplicity of the equations, we will use country indices only when it is necessary to emphasize the difference between the countries. We normalize the price index of the consumption composite to one. Thus, the budget constraint corresponding to (A2) for every adult in each country is given by:

$$c_t = \left(1 - \sum_{k=s,u} \tau_i^k n_t^k\right) w_t. \quad (\text{A4})$$

where τ_i^k is the fraction of time that a parent spends on raising a child of skill level k in country i . We assume that raising high-skilled children is costlier than raising low-skilled children ($\tau^s > \tau^u$).

The maximization of (A2) subject to (A4) yields:

$$c_t = (1 - \gamma) w_t \quad (\text{A5})$$

$$\sum_{k=s,u} \tau_i^k n_t^k = \gamma. \quad (\text{A6})$$

Equation (A6) encapsulates the quantity-quality trade-off. Because $\tau^s > \tau^u$ and the total time devoted to raising children is fixed (or increasing at a slower rate than population growth), individuals must decide between investing in smaller number of children but with higher skills and higher potential income and having a greater number of total children with lower skills and lower potential income. Therefore, in moving from an agricultural to non-agricultural society, each country is basically substituting its cheap low-skilled labor with expensive high-skilled labor. This means that the trade-off between population growth and human capital development is embedded at the heart of the model which can explain some of the inconsistencies between our results and the SSP projections.

Also, for individuals in country i to have both types of children, it must be the case that:

$$\tau_i^r = \frac{\tau_i^s}{\tau_i^u} = \frac{\sum_{j=1}^I \beta_{ij,t}^s w_{t+1}^{j,s}}{\sum_{j=1}^I \beta_{ij,t}^u w_{t+1}^{j,u}}. \quad (A7)$$

This equation shows that the ratio of expected wages of children is equal to the ratio of child rearing and migration costs.

Appendix C.2. Consumption

Total consumption by the labor of skill level k is a constant elasticity of substitution (CES) function given by:

$$c^k = \{\alpha(c_a^k)^{\frac{\epsilon-1}{\epsilon}} + (1-\alpha)(c_b^k)^{\frac{\epsilon-1}{\epsilon}}\}^{\frac{\epsilon}{\epsilon-1}}, \quad (A8)$$

where ϵ is the elasticity of substitution, c_a is consumption of the agricultural good, c_b is consumption of the non-agricultural good, and the time subscripts have been suppressed for convenience. As ϵ approaches zero, consumers get less satisfaction from substituting non-agricultural goods for agricultural goods. In the limit, there is no substitution and the goods are consumed in fixed proportions. The consumer optimization problem conditioned on the budget constraint can be formulated using the Lagrangian multiplier λ :

$$\text{Max} \left\{ c^k - \lambda (p_a c_a^k + p_b c_b^k - (1-\gamma)w^k) \right\}, \quad (A9)$$

where p_b and p_a are the prices of non-agricultural and agricultural goods, respectively. The solution to this optimization problem provides a relationship between these prices:

$$\frac{p_b}{p_a} = \left(\frac{1-\alpha}{\alpha} \right) \left(\frac{c_b^k}{c_a^k} \right)^{\frac{-1}{\epsilon}}, \quad (A10)$$

Appendix C.3. Production

We adopt a linear production functions that captures the fact that agricultural production is relatively less skill-intensive [47,48]. In this respect, our model can be therefore seen as a simplified version of the sectoral migration model of [50]. Specifically,

$$Y_b = D_b(T) A_b L^s \quad (A11)$$

$$Y_a = D_a(T) A_a L^u, \quad (A12)$$

where Y_{κ} , $\kappa = a, b$ is output in sector κ , and L^k , $k = s, u$ is total labor of skill level k . Since the only endogenous factor in the production is labor, within country inequality will be entirely driven by the composition of population which is directly impacted by migration. Total factor of productivity (TFP) or technological change is defined as A_{κ} , $\kappa = a, b$ and $D_{\kappa}(T)$ is the climate impact function for sector κ at temperature T . In order to analyze the effect of climate change in our model, we use RCP temperature projection data for each country (see the global projections in figure A1) to calculate sector-specific impact function:

$$D_{\kappa}(T) = \max \{ g_{\kappa,0} + g_{\kappa,1}T + g_{\kappa,2}T^2, D_{\kappa}^{\min} \}, \quad \kappa = a, b, \quad (A13)$$

where $g_{b,0} = 0.3$, $g_{b,1} = 0.08$, $g_{b,2} = -0.0023$, $g_{a,0} = -2.24$, $g_{a,1} = 0.308$, and $g_{a,2} = -0.0073$. The constant D_{κ}^{\min} guarantees the minimum level of economic output at very high climate damages. For our analysis we assume that $D_{\kappa}^{\min} = 10\%$. The damage function thus has the shape of a quadratic function with an optimal temperature between 17.4 (non-agricultural) and 21.1 (agriculture) degrees Celsius, and with a maximum productivity loss of 90%. The shape of this function is depicted in figure A1.

Technological change evolves exogenously according to:

$$A_{\varkappa,t} = (1 + g_{\varkappa})A_{\varkappa,t-1}, \quad \varkappa = a, b. \quad (\text{A14})$$

Total number of high-skilled and low-skilled workers are calculated by taking into account the possibility of labor movement to and from the country of interest. For example the total number of labor of skill level k in a receiving country j will be:

$$L_{j,t+1}^k = \sum_{i=1}^I N_{i,t} n_{i,t}^k \beta_{ij,t+1}^k \quad (\text{A15})$$

where $N_{i,t}$ is adult population in country i at time t . Wages can be calculated by taking the derivative of equations A11 and A12:

$$w^s = p_b D_b(T) A_b \quad (\text{A16})$$

$$w^u = p_a D_a(T) A_a, \quad (\text{A17})$$

The consumption of good type \varkappa in country i by adults of each skill level is calculated by following equations:

$$c_{i,\varkappa}^u = \frac{Y_{i,\varkappa}}{L_i^s \tau^r + L_i^u}, \quad c_{i,\varkappa}^s = c_{i,\varkappa}^u \tau^r. \quad (\text{A18})$$

Appendix C.4. Inequality

We can calculate the income inequality within each country by constructing a two-segment Lorenz curve based on empirical data. First, we obtain country quintiles (\hat{q}_i^g for quintile g in country i) from the SWIID database [52] and population $N_{k,i}$ and GDP data $Y_{k,i}$ from the World Development Indicators. Then a five segment Lorenz curve LC based on the country quintiles is approximated by a two-segment curve where we compute the share of low-skilled labour $LC(L_i^u/N_i)$ resulting in the average wages \hat{w}_i^u for the low-skilled labor and \hat{w}_i^s for high-skilled labor in country i matching GDP and the Lorenz curve at the point (L_i^u/N_i) . The inequality within a country can hence be expressed also as the wage ratio of high-skilled to low-skilled labor ($\frac{w^s}{w^u}$). Inequality across countries is calculated for each skill level separately (z^u and z^s for low-skilled and high-skilled labor respectively). For example, for high-skilled labor, it is the ratio of high-skilled wages in each country to the arithmetic average of high-skilled wages in all countries, and therefore for any country i we have

$$z^u = \frac{w^u}{(\sum_{j=1}^J w_j^u) / J} \quad (\text{A19})$$

$$(\text{A20})$$

$$z^s = \frac{w^s}{(\sum_{j=1}^J w_j^s) / J} \quad (\text{A21})$$

Appendix C.5. Equilibrium

Combining equations A10, A16, and A17 with individual maximization and production yields the following equilibrium result for each country:

$$\ln\left(\frac{L_{t+1}^s}{L_{t+1}^u}\right) = \epsilon \ln\left(\frac{1-\alpha}{\alpha}\right) - \epsilon \ln\left(\frac{w_{t+1}^s}{w_{t+1}^u}\right) - (1-\epsilon) \ln\left(\frac{D_{b,t+1}(T)}{D_{a,t+1}(T)}\right) - (1-\epsilon) \ln\left(\frac{A_{b,t+1}}{A_{a,t+1}}\right). \quad (\text{A22})$$

Note that we have used the time index $t+1$ to highlight the fact that this equation is solved by parents (i.e. adults at time t) to calculate the number of their children (i.e. adults at

time $t + 1$). Therefore, the high-skilled and low-skilled number of children at time t is corresponding to L_{t+1}^s and L_{t+1}^u (number of adults in time $t + 1$). Solving equations A6 and A22 together will give parents the optimal number and skill level of the children. The only unknown in these equations is the ratio of future wages of children $\frac{w_{t+1}^s}{w_{t+1}^u}$ which is in fact the expected wages of the children in the future and can be approximated by the current wage ratio of parents at time t . Therefore, the equilibrium equation will be rewritten as

$$\ln\left(\frac{n_t^s}{n_t^u}\right) = \epsilon \ln\left(\frac{1-\alpha}{\alpha}\right) - \epsilon \ln\left(\frac{w_t^s}{w_t^u}\right) - (1-\epsilon) \ln\left(\frac{D_{b,t+1}(T)}{D_{a,t+1}(T)}\right) - (1-\epsilon) \ln\left(\frac{A_{b,t+1}}{A_{a,t+1}}\right). \quad (\text{A23})$$

Now we can calculate the number of children of each skill level in each country given the future climate trajectories and technological change. If an increase in temperature negatively affects agriculture more than manufacturing, then the ratio $\ln\left(\frac{D_b(T)}{D_a(T)}\right)$ is an increasing function of temperature T . As the relative climate change impacts on agricultural productivity increases in developing countries, the price of agricultural goods increases [53,54]. In the absence of explicit mechanism for trade between countries, the current model treats each country as a closed economy. Therefore, given that the substitution between goods is sufficiently low ($\epsilon < 1$), any increase in the relative price of agricultural output directly translates into an increase in the relative wages of low-skilled labor working in the agricultural sector. Without migration, this raises the relative return to working in agriculture, causing parents to have relatively more low-skilled children. However, when migration possibility is taken into account, there will be a parallel movement of human capital between countries from those with lower wages to the ones with higher wages. The interaction of these two movements within each country and between countries defines the optimal level of population at end of each period.

Appendix C.6. Calibration

The model was calibrated with SSP projection data on the ratio of high-skilled to low-skilled labor in 21st century. We choose parameters to match demographic projections for each country. Historical data on migration are used to calibrate the migration probabilities.

We use several parameter values presented in [51] for other equations in the OLG model. We take $\epsilon = 0.75$ and $\alpha = 0.55/2$. We normalize the total time spent on raising children to $\gamma_0 = 45\%$ of total adult time in year 1980 for all countries. We assume the goods are complementary and therefore the values of the elasticity of substitution remain below one.

We calibrate the model to find the ratio of productivities in the beginning and end years, 2000 and 2040, as well as τ^s , τ^u , g_b , and g_a . To do so, for each country we use historical population data in year 2000 (i.e., population growth rate between 1980 and 2000, r_{2000} , and the skill ratio in 2000, h_{2000}), and the projected skill ratio in year 2040 (h_{2040}) from the Wittgenstein Centre [55]. Figure A2 shows the underlying assumptions in SSP scenarios with regard to adult population, skill ratio, GDP per capita, and Gini index throughout the century. In this paper we only use the country-level projections of skill ratio for calibrating our model.

Even though we do not directly use SSP migration projections in our model, they have been already taken into account in the calculation of the future skill ratios. To reduce the impact of this bias in the calibration of our model, we devise two remedies. First, instead of following the skill ratio trajectory in all intermediate points, we only use a single projection point for our calibration. Second, instead of using the end-of-the-century point (year 2100) we use a middle-of-the-century point (year 2040) as our projection point. This way, we allow the model to run less constrained by the SSP migration-induced biases in the second half of the century. Although a perfect remedy would be to correct the projected skill ratio for the migration numbers in each SSP, the available reported SSP migration projections are total numbers without skill differentiation [56] and therefore, the full neutralization of

migration data would require additional assumptions about the skill ratio of migration flows.

We treat anyone with a high school education and higher as high-skilled labor. Moreover, we compute initial wages by constructing a Gini coefficient for each country and, based on high- and low-skilled labor population shares, we compute the relative wages to match the regional empirical Gini coefficient in 2000 (based on the World Development Indicators). To construct the empirical Gini coefficient we use the skill ratio of each country in year 2000 (h_{2000}) to find the wages of high-income and low-income sections of the society. For example, if the skill ratio in year 2000 is $h_{2000} = \frac{2}{3}$, we assume this will be translated to $\psi_0^u = \frac{1}{1+h_{2000}} = 60\%$ share of low-income population, and $\psi_0^s = \frac{h_{2000}}{1+h_{2000}} = 40\%$ share of high-income population. The average wages of each group is calculated using the quintile data from the World Bank. The respective wages of low-skilled and high-skilled labor is calculated from equations below

$$w_0^u = \frac{\sum_{i=1}^{5 \times \psi_0^u} q_i \times Y_{2000}}{N_{2000}}, \quad (A24)$$

$$w_0^s = \frac{\sum_{i=5 \times \psi_0^u + 1}^5 q_i \times Y_{2000}}{N_{2000}}. \quad (A25)$$

where q_i is the income quintile i , Y_{2000} is the GDP, and N_{2000} is the adult population in year 2000. For each country we assume that in year 2000, equation A7 holds in its simplified form $\frac{\tau^s}{\tau^u} = \frac{w^s}{w^u} = w_{r0}$, where w_{r0} is the initial wage ratio of high-skilled to low-skilled labor. We solve the following two equations to obtain the time cost of raising children, (τ^u) and (τ^s):

$$\tau^u = \gamma \frac{1 + h_{2000}}{(1 + r_{2000})(1 + h_{2000} \times w_{r0})}, \quad (A26)$$

$$\tau^s = \tau^u \times w_{r0}. \quad (A27)$$

where r_{2000} is the adult population growth rate between the years 1980 and 2000. Next, we use equation (A23) to solve for the ratio of the initial and final technology levels, $A_{r,2000} = \frac{A_{b,2000}}{A_{a,2000}}$ and $A_{r,2040} = \frac{A_{b,2040}}{A_{a,2040}}$ assuming that the ratio of climate impacts is fixed at its year 2000 level ($D_{r0} = \frac{D_{b,2000}}{D_{a,2000}}$) and the wage ratios stay at w_{r0} level for each country. The skill ratio in year 2040 is taken from each SSP projection for each country.

$$\ln(A_{r,2000}) = \frac{\epsilon}{1-\epsilon} \ln\left(\frac{1-\alpha}{\alpha}\right) - \frac{\epsilon}{1-\epsilon} \ln(w_{r0}) - \ln(D_{r0}) - (1-\epsilon) \ln(h_{2000}) \quad (A28)$$

$$\ln(A_{r,2040}) = \frac{\epsilon}{1-\epsilon} \ln\left(\frac{1-\alpha}{\alpha}\right) - \frac{\epsilon}{1-\epsilon} \ln(w_{r0}) - \ln(D_{r0}) - (1-\epsilon) \ln(h_{2040}) \quad (A29)$$

Finally, we find the technology growth rates. By assumption, the growth rate of $\frac{A_b}{A_a}$ is constant:

$$\frac{A_{b,2040}}{A_{a,2040}} = (1 + g_r)^{\frac{(2040-2000)}{20}} \frac{A_{b,2000}}{A_{a,2000}}, \quad (A30)$$

where g_r is the growth rate of the technology ratio. It is also the only unknown variable in this equation and satisfies also

$$1 + g_r = \frac{1 + g_b}{1 + g_a}, \quad (A31)$$

where g_b is the growth rate of A_b and g_a is the growth rate of A_a . Noting that large developed countries, which have nearly all production in manufacturing, grow at much higher rate, we set $g_b = 0.1$ per year for developed counties and $g_b = 0.001$ per year for developing counties. Now, g_a can be extracted from equation (A31).

Appendix C.7. Solution algorithm

We can solve the model using a series of dynamic equations in order. First, given the the temperature projections of each RCP scenario we can calculate the damages from equation A13. Next, we calculate the exogenous component of technology using equation (A14). All of the economic decisions are captured by equation (A23), which can now be solved for the ratio of high-skilled to low-skilled individuals in every period. We can then solve for the level of the population such that equation A6 holds⁴.

The OLG model solution algorithm can be summarized as following:

1. Calibrate the exogenous growth rate of productivity for each country based on the year 2000's population and the year 2040's projected skill ratio (equations A26 to A31)
2. Run the model through time from year 2000 to year 2100 with 20-year intervals
 - (a) Calculate the number of children and their education levels for all countries. For each country, solve the parents' utility optimization problem given the current wage ratios of high-skilled to low-skilled labor and the projections of technology growth and climate impacts in different sectors (equations A6 and A23)
 - (b) Calculate the bilateral migration probabilities for every pair of countries using their current population, wages, and distance according to equation A1.
 - (c) Redistribute the next generation's population calculated in step (a) according to the migration probabilities obtained in step (b)
 - (d) Update the next generation's population and skill ratio and calculate the economic output, wages for the next time step

$$\ln\left(\frac{w_{t+1}^s}{w_{t+1}^u}\right) = \ln\left(\frac{1-\alpha}{\alpha}\right) - \frac{1}{\epsilon} \ln\left(\frac{L_{t+1}^s}{L_{t+1}^u}\right) - \frac{1-\epsilon}{\epsilon} \ln\left(\frac{D_{b,t+1}(T)}{D_{a,t+1}(T)}\right) - \frac{1-\epsilon}{\epsilon} \ln\left(\frac{A_{b,t+1}}{A_{a,t+1}}\right) \quad (A32)$$

These wages will be used to calculate the probability of migration in the next period as well as the utility optimization that the parents in next generation use to find the optimal skill ratio of their children (equation A23). Therefore, the impacts of migration on local wages can influence the wage inequality and migration patterns in next periods.

Appendix D. Alternative setups

In this section we report the results of some modifications in the model and its assumptions along with some robustness checks and sensitivity analysis.

Appendix D.1. PPML migration probability estimation

The PPML model replicates the probability estimation based on [6] and [26].

$$\frac{M_{ij,t+1}^k}{L_{i,t+1}} = \exp\left[\theta_1^k \log(L_{i,t}^k) + \theta_2^k \log(L_{j,t}^k) + \theta_3^k \log\left(\frac{GDPPC_{j,t}^k}{GDPPC_{i,t}^k}\right) + \theta_4^k \log(d_{ij}) + \eta_i + \delta_j\right] \varepsilon_{ij}^k \quad (A33)$$

The results of this alternative setup are presented in table A3. Although this model is better in dealing with historical migration panel data that contain large amount of zero values and will give a better estimate of historical migration trends, its application in the OLG model for estimating future migration probabilities very limited. The main reason is the exponential function on the right hand-side that inflates any changes in the scale of the variables and radically increases the probability on the left hand-side.

For example, we run the OLG model under RCP2.6 and SSP1 (very mild inequality and climate conditions). We observe that the exponential form of the probability function

⁴ we assume an increase of 5% in child-rearing costs for both types of children globally in each period based on the evidence suggesting an increase in parenting time in selected countries [57]

Table A3. Migration Gravity Model estimation (PPML)

	Pooled	High-skilled	Low-skilled
$\log(L_i)$	-0.23 (0.17)	-0.20 (0.18)	0.80** (0.25)
$\log(L_j)$	-1.51*** (0.22)	-1.01*** (0.23)	-0.09 (0.18)
$\log\left(\frac{GDPPC_j}{GDPPC_i}\right)$	0.75*** (0.10)	0.63** (0.22)	0.34*** (0.08)
$\log(d_{ij})$	-0.24*** (0.01)	-0.24*** (0.01)	-0.24*** (0.01)
Num. obs.	25117	15629	15629

All estimations include origin and destination fixed effects.

Table A4. Probability of high-skilled (h) migration from Colombia to Spain and to the USA with PPML estimation.

Period	Destination	constants	$\theta_1^h L_i^h$	$\theta_2^h L_j^h$	$\theta_3^h \frac{w_j^h}{w_i^h}$	sum	Probability
2000-2020	Spain	20.215	-3.279	-17.009	0.759	0.686	0.198%
	USA	24.078	-3.279	-19.259	0.889	2.429	1.135%
2020-2040	Spain	20.215	-3.387	-17.208	1.971	1.591	0.491%
	USA	24.078	-3.387	-19.491	2.057	3.257	2.597%
2040-2060	Spain	20.215	-3.397	-17.125	3.163	2.856	1.739%
	USA	24.078	-3.397	-19.663	3.236	4.254	7.039%
2060-2080	Spain	20.215	-3.342	-16.917	4.353	4.309	7.437%
	USA	24.078	-3.342	-19.761	4.422	5.397	22.074%
2080-2100	Spain	20.215	-3.213	-16.699	5.545	5.848	34.654%
	USA	24.078	-3.213	-19.814	5.614	6.665	78.446%

has a large impact on the migration probabilities of smaller countries in later years during the simulation. We take the high-skilled (h) migration from Colombia to Spain and to the USA as an example and investigate how these migration probabilities evolve over time. The results of our analysis are shown in table A4. As it is shown, the high-skilled migration probability to Spain increases drastically from about 0.2% in the 2000-2020 period to nearly 34.7% in the last period. Meanwhile, the high-skilled migration probability from Colombia to the USA starts at around 1.1% and reaches to about 78.4%. As a result of just these two migration probabilities, the total migration probability exceeds one and makes the model's calculation of population and migration flows infeasible. Therefore, we rule out PPML model as an appropriate estimation model for our migration projection and instead we use the OLS model with logarithmic terms as described in the manuscript as the main estimation model. The results of the OLS calculation for the same example are shown in table A5.

Appendix D.2. Migration policy

SSP scenarios come with different narratives about international migration [58] that cannot be reflected in our OLG model without introducing additional assumptions. For example, high inequality assumptions in SSP3 and SSP4 scenarios translates into high bilateral migration flows following the equation (A1). However, these SSP scenarios have strong assumptions about regional rivalry and stricter migration policies which cannot be captured by this model. In order to adjust the scale of international migration flows and make them consistent with SSP narratives, one can introduce an ad-hoc policy parameter which applies universally to all bilateral migration probabilities. Therefore, we can modify

Table A5. Probability of high-skilled (h) migration from Colombia to Spain and to the USA with OLS estimation.

Period	Destination	constants	$\theta_1^h L_i^h$	$\theta_2^h L_j^h$	$\theta_3^h \frac{w_j^h}{w_i^h}$	sum	Probability
2000-2020	Spain	8.547	2.819	-6.438	0.204	5.132	0.513%
	USA	18.287	2.819	-7.289	0.239	14.056	1.406%
2020-2040	Spain	8.547	2.908	-6.519	0.529	5.465	0.547%
	USA	18.287	2.908	-7.390	0.553	14.358	1.436%
2040-2060	Spain	8.547	2.910	-6.500	0.849	5.806	0.581%
	USA	18.287	2.910	-7.470	0.869	14.596	1.460%
2060-2080	Spain	8.547	2.864	-6.440	1.169	6.140	0.614%
	USA	18.287	2.864	-7.515	1.187	14.823	1.482%
2080-2100	Spain	8.547	2.786	-6.358	1.489	6.464	0.646%
	USA	18.287	2.786	-7.532	1.507	15.048	1.505%

the migration probability equation to account for underlying migration policy differences between SSP scenarios:

$$\beta_{ij,t+1}^k = \left[\theta_{ij}^k + \theta_1^k \log(L_{i,t}^k) + \theta_2^k \log(L_{j,t}^k) + \theta_3^k \log\left(\frac{w_{j,t}^k}{w_{i,t}^k}\right) + \theta_4^k \log(d_{ij}) + \eta_i + \delta_j \right] \times (1 - \zeta_{ij}^{ssp}), \quad (\text{A34})$$

where parameter $0 \leq \zeta_{ij}^{ssp} \leq 1$ is the relative cost of migration of labor of skill level k from country i to j reflecting the restrictiveness of policies that govern the migration of labor from country i to j under a given ssp scenario. When this parameter is zero, we assume no restriction in labor mobility, while the value equal to 1 means absolute closure of the borders. Within the SSP framework and for all pairs of countries, we assume $\zeta_{ij}^{ssp} = 0.5$ for SSP1, SSP2, and SSP4 where international migration is *medium*, $\zeta_{ij}^{ssp} = 0.1$ for SSP5 where international migration is *high*, and $\zeta_{ij}^{ssp} = 0.9$ for SSP3 where international migration is *low*. Figure A3 shows the impact of the introduction of this parameter in the model on total migration flows across SSP scenarios.

As expected, the introduction of $\zeta_{ij}^{ssp} = 0.5$ reduces the migration flows by about 50% under SSP1, SSP2, and SSP4 scenarios, while migration flows under SSP5 remain almost unchanged. On the other hand, the introduction of $\zeta_{ij}^{ssp} = 0.9$ for SSP3 reduces the migration flows drastically and results in an early collapse of migration flows in year 2020.

Appendix D.3. RCP2.6 scenario

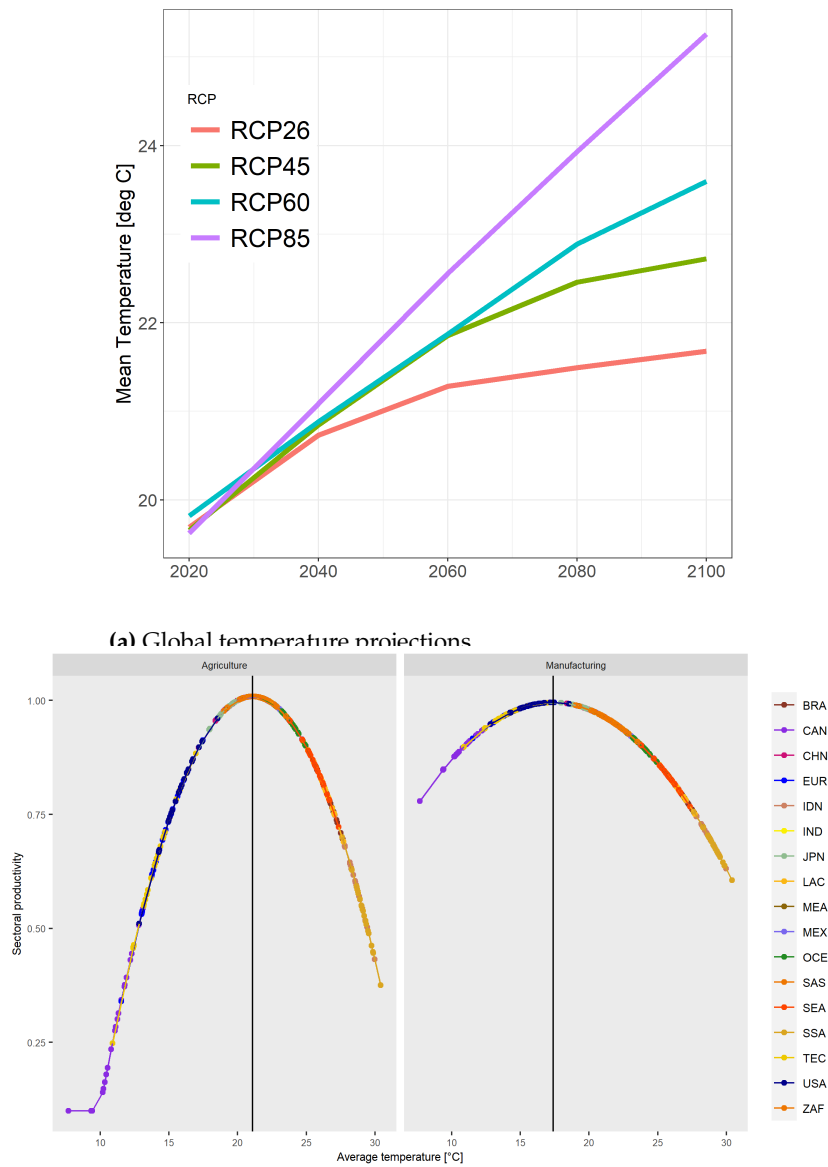
In order to distinguish the impact of climate change on international migration under each SSP, We consider two RCP cases with different temperature trajectories (see panel (a) in figure A1). For the *baseline case* we allow for temperatures to change according to the RCP6.0 projections and therefore, migration will be affected indirectly by climate change through its impact on wages. The second case is based on a low-risk climate change scenario of RCP2.6 where we assume that climate change is limited and the migration will be marginally impacted. The results of the *baseline case* are presented in the main manuscript. Here we provide additional results mainly based on the RCP2.6 case.

First, we consider the total migration flows over time presented in panel (a) in figure A4. The patterns are similar to the *baseline case* in the main manuscript. In both cases, total migration in the SSP1, 2, and 5 scenarios demonstrates an initial increase through the middle of the century and a downward trend afterwards. In the SSP3 and SSP4 scenarios however, widespread inequality will drive international migration flows to their pick by the end of the century. The global flow of high-skilled migrants follows similar pattern for all the SSP scenarios as it is shown in panel (b) in figure A4. However, the global flow of

low-skilled migrants decreases under SSP1, 2, and 5 scenarios while increasing under SSP3 and SSP4 scenarios as it is shown in panel (c) in figure [A4](#).

In terms of regional hot spots, India emerges as a big sending country while Europe keeps its position as an attractive destination and the US role a major receiving country declines. Figure [A5](#) shows the breakdown of migration flows between and inside regions and across SSPs for the RCP2.6 case.

Figures [A6](#) and [A7](#) show the breakdown of total migration flows in 2100 by region across SSP scenarios for the RCP26 case and *baseline case* respectively.



(b) Damage function

Figure A1. Global projections of temperature and climate change damages for agricultural and non-agricultural sector (sectoral efficiency for different temperatures) based on [51].

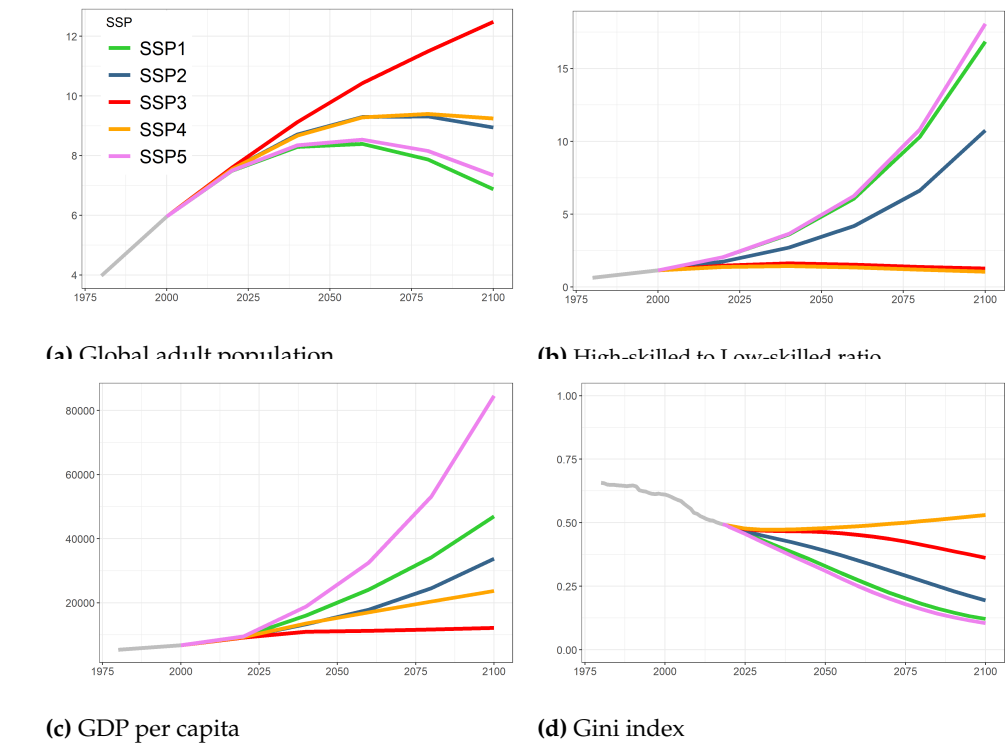


Figure A2. Global socioeconomic indicators under different SSP scenarios from [34].

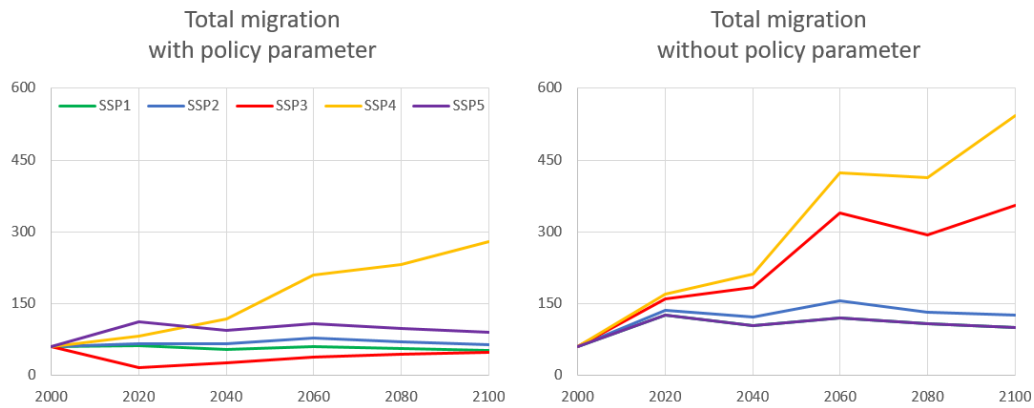


Figure A3. The impact of policy parameter on total migration flows across SSP scenarios.

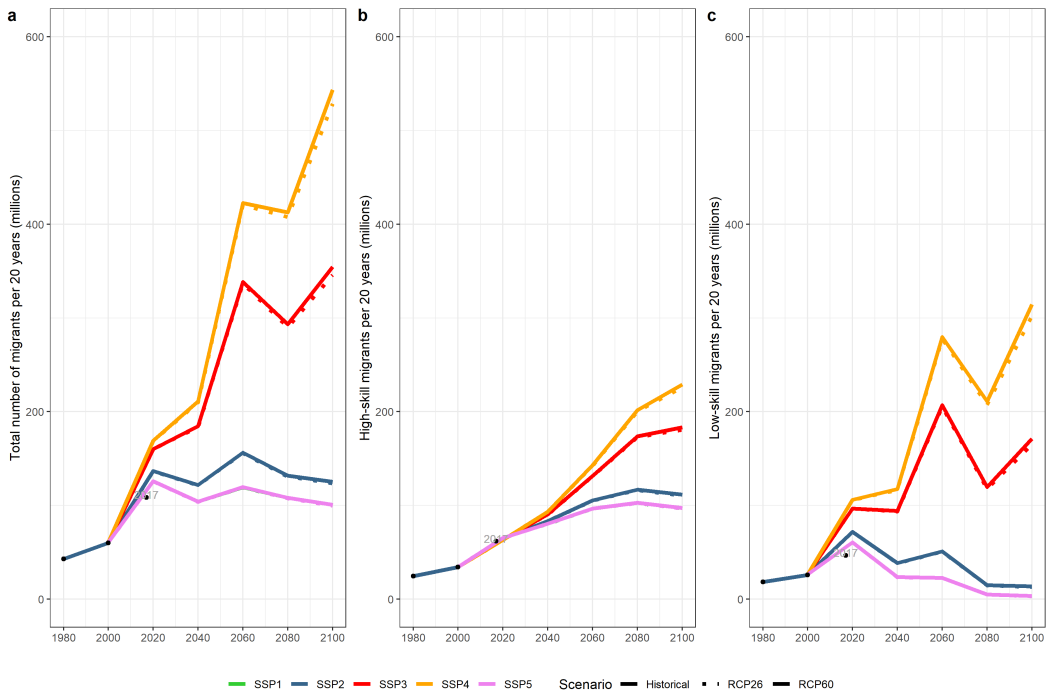


Figure A4. Historical and projections of twenty-year global migration flows for RCP2.6 and RCP6.0 cases. (a) Total global migration. (b) High-skilled global migration. (c) Low-skilled global migration.

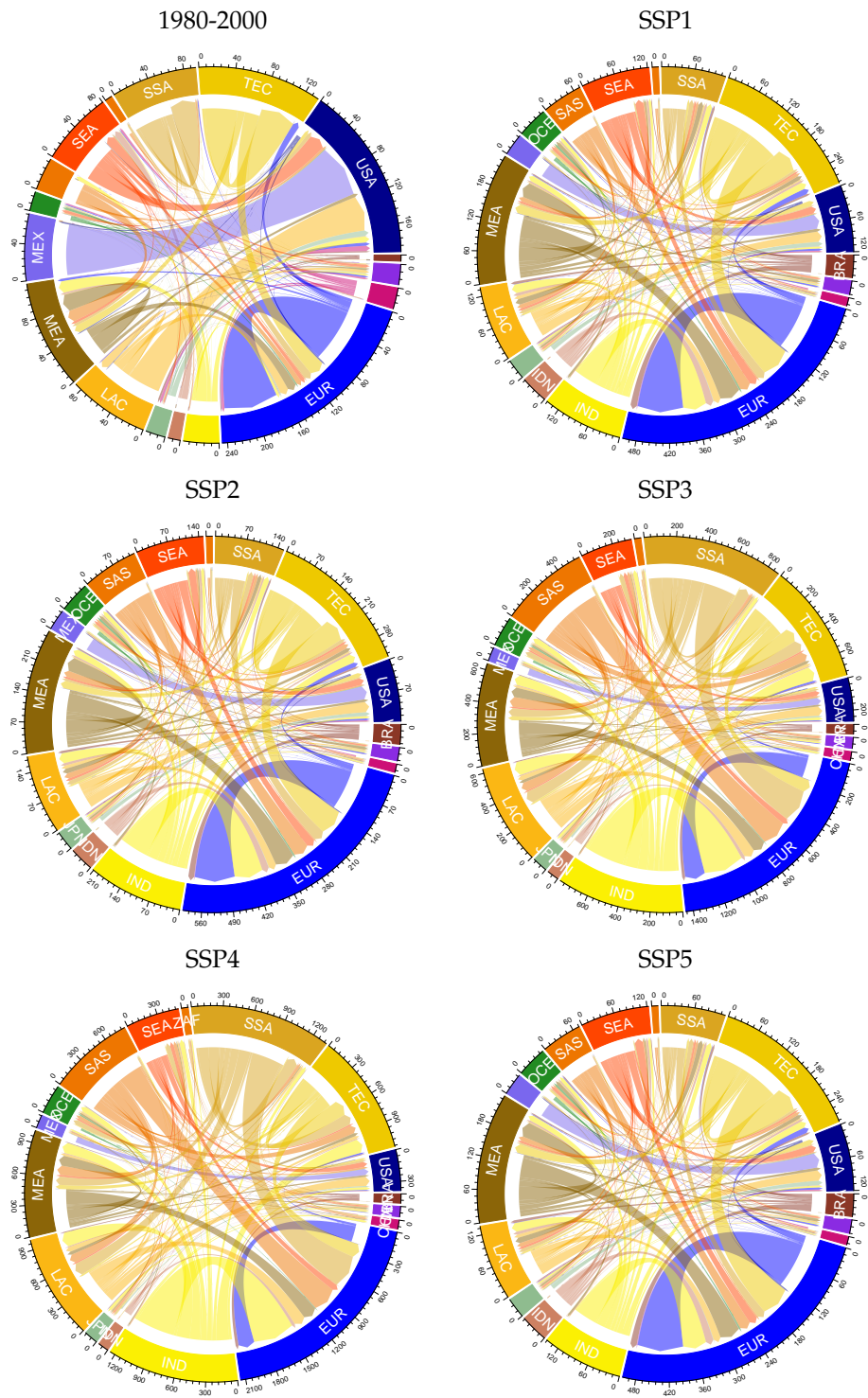


Figure A5. Regional bilateral migration flows, between 2080 and 2100, annually in 100 thousands under RCP2.6

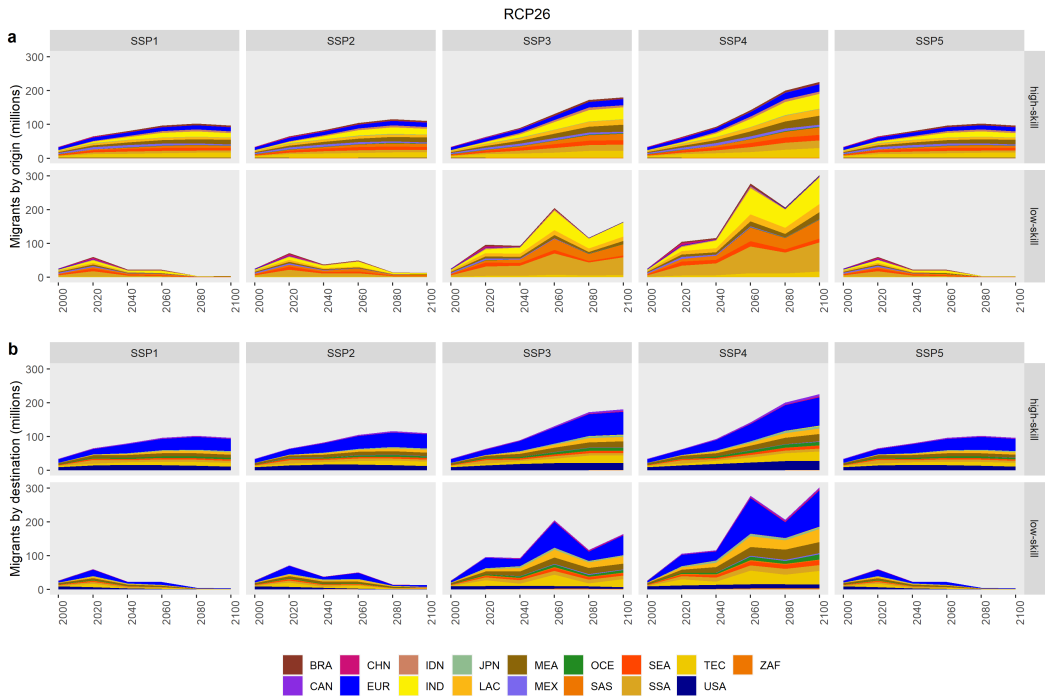


Figure A6. Migration flows of high-skilled and low-skilled labor under RCP2.6 case: (a) distribution of migrants by origin, and (b) distribution of migrants by destination.

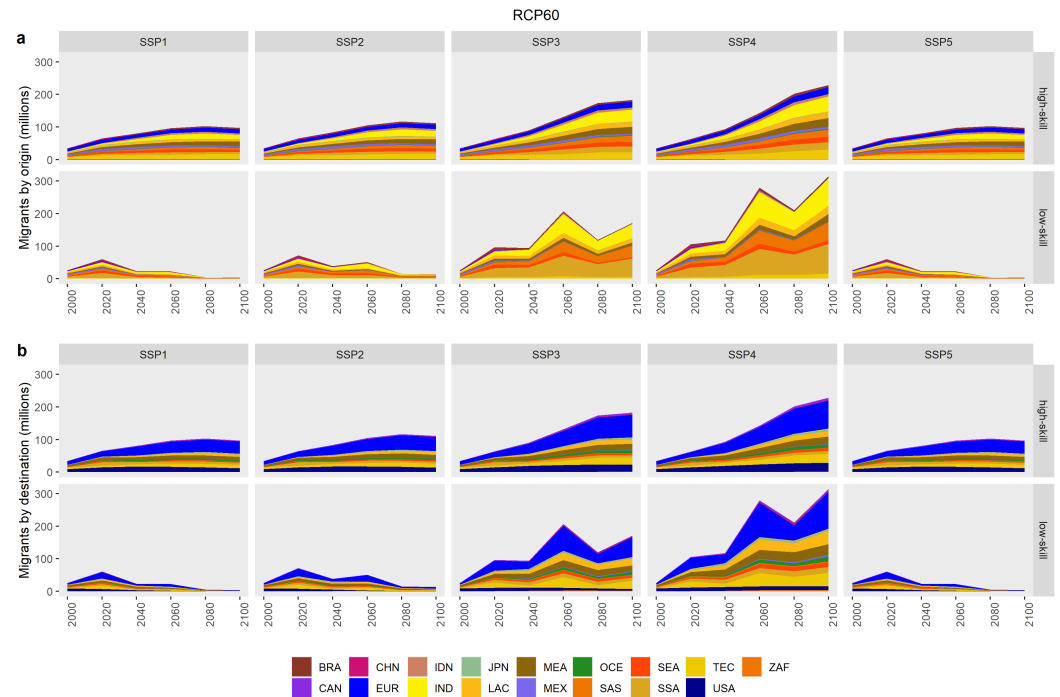


Figure A7. Migration flows of high-skilled and low-skilled labor under RCP6.0 case: (a) distribution of migrants by origin, and (b) distribution of migrants by destination.

Panel (a) in Figure A8 shows the change in human capital accumulation across the SSPs for the RCP2.6 case. In SSP1, SSP2, and SSP5 the population of high-skilled labor compared to low-skilled labor increases dramatically towards the end of the century due to a global education push. In contrast, the ratio of high-skilled to low-skilled labor does not increase as fast in SSP3 and SSP4. Panel (b) in Figure A8 shows the percentage change in the high-skilled, low-skilled, and total adult population in the *baseline* case compared to the RCP2.6 case. In all scenarios, the low-skilled labor has a fast increasing trend while the high-skilled population is increasing in a much smaller pace.

Appendix D.4. Climate change foresight

Climate change foresight is one of the key determinants of fertility and child education decisions as shown by the relative productivity ratio ($\frac{D_{b,t+1}(T)}{D_{a,t+1}(T)}$) in equation (A22). Although the underlying assumption here is that the parents can foresee the upcoming climate changes and internalize such signals in their fertility decisions, it might be hard to justify the reality of such assumption in the real world. In order to check the robustness of our results against this assumption, we modify the model to use the parents' realization of the productivity ratio due to climate damages at the current time ($\frac{D_{b,t}(T)}{D_{a,t}(T)}$) instead of the projected ratio in the next period. We run the model under RCP2.6 and RCP6.0 climate change scenarios. The results for the total population, global skill ratio, and global migration flows are reported in three panels of table A6 as percentage change compared to the original case with perfect foresight. In the case without climate change foresight, parents in developing countries with larger agricultural sector, underestimate the future warming and therefore, will have less incentive to have higher number of low-skilled children compared to the original case with perfect climate change foresight. Therefore, the overall result is lower population, lower migration, and higher skill ratio globally in most years for most SSPs. The difference between these two cases in terms of total global population and migration flows are less than 1% in all SSP-RCP scenarios throughout the century. Although the difference in skill ratios are a bit higher, they are still under 2% under all SSP-RCP scenarios. Comparing the differences between two RCP scenarios, RCP2.6

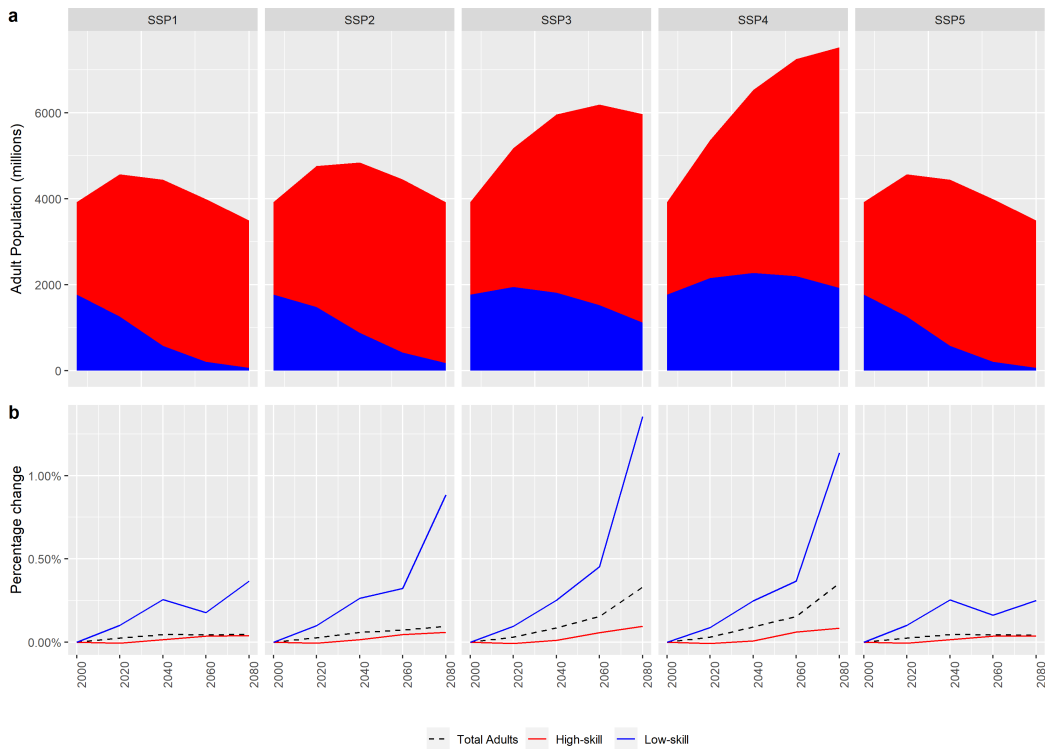


Figure A8. Human capital accumulation across the SSPs. (a) High-skilled and low-skilled adult population under RCP2.6 case. (b) Percentage change in high-skilled (red colour), low-skilled (blue colour), and total adult population (dotted line) under RCP6.0 case compared to RCP2.6 case.

with lower and RCP6.0 with higher climate change reveals that the difference between the case with perfect climate foresight and the case without climate change foresight is larger under RCP6.0 as climate change impacts are larger in this scenario.

Appendix E. Comparison with SSP migration

Table A7 shows the comparison between the results of our model and the underlying migration assumptions in the SSPs for selected countries [56] for the period 2060-2080. The numbers reflect the migration stress defined as the net number of migrants in the 20-year period as a percentage of the total adult population in year 2080. The OLG results are in general higher than the SSP assumptions however the migration signs are mostly consistent between our model and the SSP underlying assumptions.

Appendix F. Additional results

Comparing the probability of migration and migration flows across time in different SSP scenarios in figure A9 shows that

- in the SSP1, SSP2, and SSP5 scenarios although low-skilled and high-skilled migration probabilities are in the same range, high-skilled migrants are coming from a faster growing population base, and
- in the SSP3 and SSP4 scenarios, low-skilled migration probabilities are lower than high-skilled ones but low-skilled migrants are coming from countries with larger population.

Table A6. Percentage change in total (adult) population, skill ratio, and total migration under RCP2.6 and RCP6.0 scenarios in the case without climate change foresight compared to the case with climate change foresight.

Percentage change in total population		SSP1	SSP2	SSP3	SSP4	SSP5
2000	RCP2.6 RCP6.0	0.00% 0.00%	0.00% 0.00%	0.00% 0.00%	0.00% 0.00%	0.00% 0.00%
2020	RCP2.6 RCP6.0	-0.21% -0.24%	-0.22% -0.25%	-0.23% -0.26%	-0.28% -0.31%	-0.21% -0.24%
2040	RCP2.6 RCP6.0	-0.15% -0.20%	-0.15% -0.21%	-0.12% -0.20%	-0.12% -0.22%	-0.15% -0.20%
2060	RCP2.6 RCP6.0	-0.17% -0.19%	-0.16% -0.21%	-0.11% -0.23%	-0.11% -0.23%	-0.17% -0.19%
2080	RCP2.6 RCP6.0	-0.17% -0.19%	-0.16% -0.22%	-0.06% -0.33%	-0.07% -0.35%	-0.17% -0.19%
2100	RCP2.6 RCP6.0	-0.17% -0.20%	-0.16% -0.26%	-0.01% -0.47%	0.02% -0.56%	-0.17% -0.20%

Percentage change in skill ratio		SSP1	SSP2	SSP3	SSP4	SSP5
2000	RCP2.6 RCP6.0	0.00% 0.00%	0.00% 0.00%	0.00% 0.00%	0.00% 0.00%	0.00% 0.00%
2020	RCP2.6 RCP6.0	0.84% 0.95%	0.78% 0.89%	0.66% 0.76%	0.78% 0.87%	0.84% 0.95%
2040	RCP2.6 RCP6.0	-0.67% -0.40%	-0.59% -0.34%	-0.50% -0.28%	-0.62% -0.38%	-0.67% -0.41%
2060	RCP2.6 RCP6.0	-0.19% -0.13%	-0.20% -0.01%	-0.18% 0.15%	-0.19% 0.06%	-0.19% -0.15%
2080	RCP2.6 RCP6.0	0.04% 0.24%	-0.28% 0.44%	-0.54% 0.67%	-0.41% 0.61%	0.07% 0.18%
2100	RCP2.6 RCP6.0	-0.11% 1.37%	-0.60% 1.34%	-0.98% 1.19%	-0.82% 1.13%	0.04% 1.15%

Percentage change in total migration		SSP1	SSP2	SSP3	SSP4	SSP5
2000	RCP2.6 RCP6.0	0.00% 0.00%	0.00% 0.00%	0.00% 0.00%	0.00% 0.00%	0.00% 0.00%
2020	RCP2.6 RCP6.0	-0.08% -0.12%	-0.07% -0.12%	-0.06% -0.10%	-0.10% -0.14%	-0.08% -0.12%
2040	RCP2.6 RCP6.0	0.03% -0.05%	0.05% -0.06%	0.09% -0.08%	0.11% -0.07%	0.03% -0.05%
2060	RCP2.6 RCP6.0	-0.15% -0.24%	-0.24% -0.39%	-0.46% -0.71%	-0.51% -0.75%	-0.14% -0.23%
2080	RCP2.6 RCP6.0	-0.02% -0.11%	-0.01% -0.19%	0.03% -0.49%	0.01% -0.61%	-0.01% -0.11%
2100	RCP2.6 RCP6.0	-0.03% -0.19%	-0.03% -0.36%	-0.08% -1.03%	-0.05% -1.18%	-0.03% -0.17%

Table A7. Comparison of the SSP migration assumptions [56] with the results of the OLG model for selected countries. The values show the 20-year net migration stress (percentage of net migration in total adult population) for the period 2060-2080

Country		SSP1	SSP2	SSP3	SSP4	SSP5
Brazil	SSP	-0.33	0.34	-0.15	-0.25	-0.66
	OLG	-7.94	-7.59	-6.91	-7.41	-7.94
China	SSP	-0.14	-0.15	-0.07	-0.11	-0.29
	OLG	0.07	0.12	0.52	0.57	0.07
Egypt	SSP	-0.60	-0.60	-0.25	-0.46	-1.20
	OLG	-9.16	-8.65	-7.32	-7.52	-9.16
Germany	SSP	3.36	3.75	2.53	4.26	4.60
	OLG	7.25	8.01	12.20	15.30	7.21
India	SSP	-0.30	-0.30	-0.13	-0.24	-0.59
	OLG	-5.42	-5.61	-6.75	-7.63	-5.42
Indonesia	SSP	-0.70	-0.69	-0.29	-0.52	-1.39
	OLG	-7.78	-7.38	-6.38	-6.52	-7.78
Mexico	SSP	-2.31	-2.32	-0.96	-1.80	-4.60
	OLG	-9.41	-8.92	-5.32	-4.90	-9.42
Nigeria	SSP	-0.45	-0.44	-0.18	-0.40	-0.90
	OLG	-6.09	-5.64	-5.58	-5.91	-6.09
Pakistan	SSP	-1.79	-1.80	-0.75	-1.69	-3.58
	OLG	-6.95	-7.40	-10.31	-11.69	-6.95
Korea	SSP	0.31	0.35	0.24	0.40	0.43
	OLG	-0.50	0.07	3.16	4.77	-0.51
Russia	SSP	2.19	2.84	2.41	3.13	2.80
	OLG	0.28	0.67	2.30	2.29	0.28
South Africa	SSP	2.06	2.75	2.35	3.03	2.62
	OLG	-0.90	-0.27	3.15	3.72	-0.90
USA	SSP	3.15	3.54	2.42	4.09	4.27
	OLG	3.90	4.42	6.98	8.83	3.91

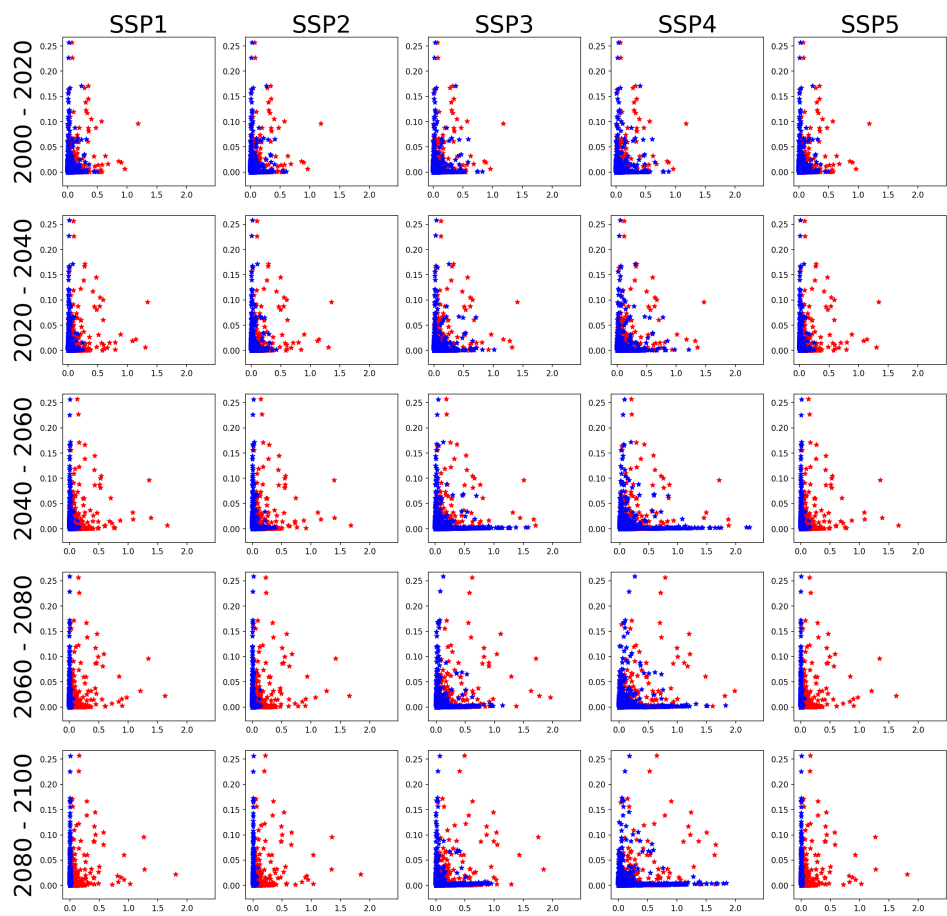


Figure A9. Evolution of bilateral migration flows in million people (X-axis) and migration probabilities (Y-axis) across time and SSPs. Migration flow between each pair of countries is represented by two dots: high-skilled migration in red and low-skilled migration in blue.

As a result, high-skilled migration is more dominant in SSP1, SSP2, and SSP5 while low-skilled migration is larger in SSP3 and SSP4 highlighting the fact that *inequality effect* is more dominant among low-skilled migrants.⁵

Finally, the flow of bilateral migration can exert population stress in both sending and receiving countries. The ratio of migrants to adult populations of sending and receiving countries under the five SSP scenarios is depicted in figure A10 for the 2060-2080 period. Comparing the historical stress levels from the 1980-2000 period with the future projections also reveals that although some of historical destinations like North America and Europe will continue to attract international immigrants, new regional hot-spots in Sub-Saharan Africa and Asia are emerging. Meanwhile India and Brazil will experience higher rate of emigration compared to the historical levels. Table A6 in section Appendix.D.4 provides a comparison between the results of our model and the underlying migration assumptions for selected countries in each SSP scenario⁶.

⁵ Some empirical studies have also shown that the number of high-skilled labor is potentially larger than the number of low-skilled migrants. The reason however, is that high-skilled workers, compared to their low-skilled counterparts, have access to greater financial resources which enable them to migrate in larger numbers [59,60].

⁶ In general, the OLG model generates larger migration ratios than the underlying SSP assumptions. There are several explanations for such discrepancies. First, the population in the OLG model is endogenous while the model follows the SSP assumptions about the growth rate of skill ratio. This leads to sharp increase in the share of high-skilled labor over the next few decades which in turn reduces the fertility in these countries. However, the SSP population growth assumptions are not necessarily held back by such trade-off. Second, we have not included any migration policy change in our baseline model. Therefore, in the absence of a detailed migration policy projection for each country and skill level, we believe our results can provide an estimated upper-bound on migration flows.

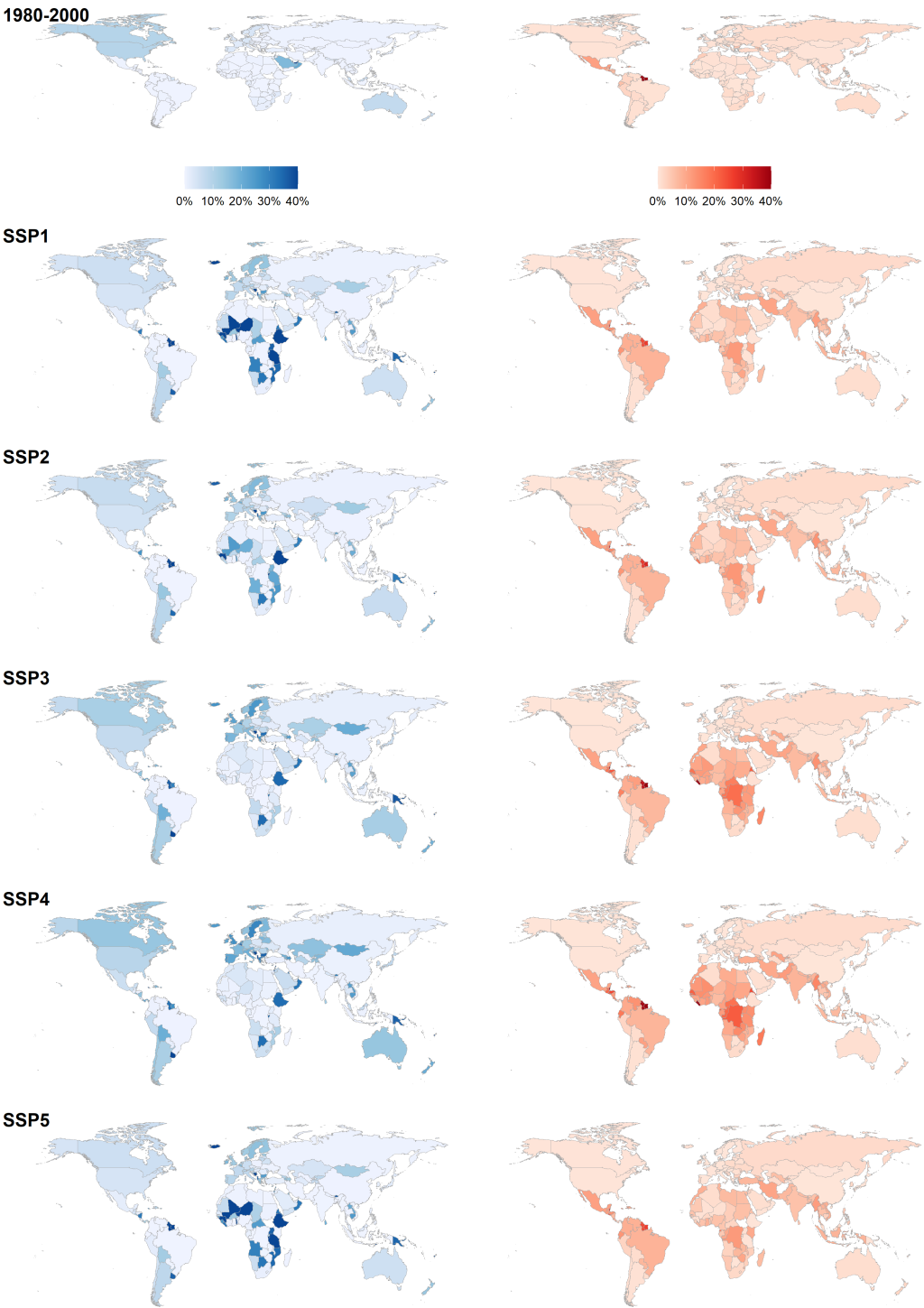


Figure A10. Ratio of migrants to adult population in receiving (blue) and sending (red) regions in the 1980-2000 and 2060-2080 periods across the SSPs.

References

1. Castles, S.; De Haas, H.; Miller, M.J. *The age of migration: International population movements in the modern world*; Macmillan International Higher Education, 2013.
2. De Haas, H.; Czaika, M.; Flahaux, M.L.; Mahendra, E.; Natter, K.; Vezzoli, S.; Villares-Varela, M. International migration: Trends, determinants, and policy effects. *Population and Development Review* **2019**, *45*, 885–922.
3. UN Department of Economic and Social Affairs. International Migration Report. Technical report, United Nations, 2017.
4. Missirian, A.; Schlenker, W. Asylum applications respond to temperature fluctuations. *Science* **2017**, *358*, 1610–1614.
5. Black, R.; Arnell, N.W.; Adger, W.N.; Thomas, D.; Geddes, A. Migration, immobility and displacement outcomes following extreme events. *Environmental Science & Policy* **2013**, *27*, S32–S43.
6. Beine, M.; Bertoli, S.; Fernández-Huertas Moraga, J. A Practitioners' Guide to Gravity Models of International Migration. *The World Economy* **2016**, *39*, 496–512. doi:10.1111/twec.12265.
7. Docquier, F.; Peri, G.; Ruysen, I. The cross-country determinants of potential and actual migration. *International Migration Review* **2014**, *48*, 37–99.
8. UN Department of Economic and Social Affairs. World Population Prospects The 2017 Revision. Technical report, United Nations, 2017.
9. Azose, J.J.; Raftery, A.E. Bayesian Probabilistic Projection of International Migration. *Demography* **2015**, *52*, 1627–1650. doi:10.1007/s13524-015-0415-0.
10. Delogu, M.; Docquier, F.; Machado, J. Globalizing labor and the world economy: the role of human capital. *Journal of Economic Growth* **2018**, *23*, 223–258. doi:10.1007/s10887-017-9153-z.
11. Docquier, F.; Machado, J. Income Disparities, Population and Migration Flows Over the Twenty First Century. *Italian Economic Journal* **2017**, *3*, 125–149.
12. Docquier, F. Long-term trends in international migration: Lessons from macroeconomic model. *Economics and Business Review* **2018**, *4*, 3–15.
13. Burzynski, M.; Deuster, C.; Docquier, F. Geography of skills and global inequality. *Journal of Development Economics* **2020**, *142*, 102333.
14. O'Neill, B.C.; Kriegler, E.; Riahi, K.; Ebi, K.L.; Hallegatte, S.; Carter, T.R.; Mathur, R.; van Vuuren, D.P. A new scenario framework for climate change research: the concept of shared socioeconomic pathways. *Climatic Change* **2014**, *122*, 387–400.
15. Burzynski, M.; Deuster, C.; Docquier, F.; De Melo, J. Climate change, inequality and migration. Technical report, Technical report, 2018.
16. Aydemir, A.; Borjas, G.J. Cross-country variation in the impact of international migration: Canada, Mexico, and the United States. *Journal of the European Economic Association* **2007**, *5*, 663–708.
17. Card, D. Immigrant inflows, native outflows, and the local labor market impacts of higher immigration. *Journal of Labor Economics* **2001**, *19*, 22–64.
18. Ruhs, M.; Vargas-Silva, C. The labour market effects of immigration. *Migration Observatory briefing, COMPAS, University of Oxford, Oxford* **2015**.
19. Ottaviano, G.I.P.; Peri, G. Rethinking the Effect of Immigration on Wages. *Journal of the European Economic Association* **2012**, *10*, 152–197. doi:10.1111/j.1542-4774.2011.01052.x.
20. Ortega, F.; Peri, G. The Causes and Effects of International Migrations: Evidence from OECD Countries 1980-2005. Working Paper 14833, National Bureau of Economic Research, 2009. doi:10.3386/w14833.
21. Black, R.; Kniveton, D.; Skeldon, R.; Coppard, D.; Murata, A.; Schmidt-Verkerk, K. Demographics and climate change: future trends and their policy implications for migration. *Development Research Centre on Migration, Globalisation and Poverty. Brighton: University of Sussex* **2008**.
22. Lutz, W.; Goujon, A.; KC, S.; Stonawski, M.; Stilianakis, N. Demographic and Human Capital Scenarios for the 21st Century: 2018 assessment for 201 countries. Technical report, Publications Office of the European Union, 2018.
23. Gemenne, F.; Blocher, J. How can migration serve adaptation to climate change? Challenges to fleshing out a policy ideal. *The Geographical Journal* **2017**, *183*, 336–347.
24. Coniglio, N.D.; Pesce, G. Climate variability and international migration: an empirical analysis. *Environment and Development Economics* **2015**, *20*, 434–468.
25. Gray, C.; Wise, E. Country-specific effects of climate variability on human migration. *Climatic change* **2016**, *135*, 555–568.
26. Ramos, R.; Suriñach, J. A Gravity Model of Migration Between the ENC and the EU. *Tijdschrift voor economische en sociale geografie* **2017**, *108*, 21–35. doi:10.1111/tesg.12195.
27. Nawrotzki, R.J.; Bakhtsiyarava, M. International climate migration: Evidence for the climate inhibitor mechanism and the agricultural pathway. *Population, space and place* **2017**, *23*, e2033.
28. Gröschl, J.; Steinwachs, T. Do Natural Hazards Cause International Migration? *CESifo Economic Studies* **2017**, *63*, 445–480.
29. Beine, M.; Parsons, C. Climatic factors as determinants of international migration. *The Scandinavian Journal of Economics* **2015**, *117*, 723–767.
30. Cai, R.; Feng, S.; Oppenheimer, M.; Pytlikova, M. Climate variability and international migration: The importance of the agricultural linkage. *Journal of Environmental Economics and Management* **2016**, *79*, 135–151.

31. Casey, G.; Shayegh, S.; Moreno-Cruz, J.; Bunzl, M.; Galor, O.; Caldeira, K. The impact of climate change on fertility. *Environmental Research Letters* **2019**, *14*, 054007.
32. Shayegh, S. Outward migration may alter population dynamics and income inequality. *Nature Climate Change* **2017**, *7*, 828.
33. Martin, S.; Weerasinghe, S.; Taylor, A. Crisis migration. *The Brown Journal of World Affairs* **2013**, *20*, 123–137.
34. Riahi, K.; van Vuuren, D.P.; Kriegler, E.; Edmonds, J.; O'Neill, B.C.; Fujimori, S.; Bauer, N.; Calvin, K.; Dellink, R.; Fricko, O.; et al. The Shared Socioeconomic Pathways and their energy, land use, and greenhouse gas emissions implications: An overview. *Global Environmental Change* **2017**, *42*, 153–168. doi:10.1016/j.gloenvcha.2016.05.009.
35. Samir, K.; Lutz, W. The human core of the shared socioeconomic pathways: Population scenarios by age, sex and level of education for all countries to 2100. *Global Environmental Change* **2017**, *42*, 181–192.
36. KC, S.; Lutz, W. The human core of the shared socioeconomic pathways: Population scenarios by age, sex and level of education for all countries to 2100. *Global Environmental Change* **2017**, *42*, 181–192. doi:10.1016/j.gloenvcha.2014.06.004.
37. Mayda, A.M. International migration: A panel data analysis of the determinants of bilateral flows. *Journal of Population Economics* **2010**, *23*, 1249–1274.
38. Rogelj, J.; Meinshausen, M.; Knutti, R. Global warming under old and new scenarios using IPCC climate sensitivity range estimates. *Nature climate change* **2012**, *2*, 248–253.
39. Biavaschi, C.; Burzynski, M.; Elsner, B.; Machado, J. Taking the Skill Bias out of Global Migration. Technical Report 201810, Geary Institute, University College Dublin, 2018.
40. IMF. World Economic Outlook Database. Technical report, IMF, 2018.
41. Dellink, R.; Chateau, J.; Lanzi, E.; Magné, B. Long-term economic growth projections in the Shared Socioeconomic Pathways. *Global Environmental Change* **2017**, *42*, 200–214. doi:10.1016/j.gloenvcha.2015.06.004.
42. Ratha, D.; Mohapatra, S.; Silwal, A. Migration and remittances factbook 2011. Technical Report 57869, The World Bank, 2010.
43. Silva, J.M.C.S.; Tenreyro, S. The Log of Gravity. *The Review of Economics and Statistics* **2006**, *88*, 641–658. Publisher: MIT Press, doi:10.1162/rest.88.4.641.
44. Adams Jr, R.H.; Page, J. Do international migration and remittances reduce poverty in developing countries? *World development* **2005**, *33*, 1645–1669.
45. Diamond, P.A. National debt in a neoclassical growth model. *American Economic Review* **1965**, *55*, 1126–1150.
46. Galor, O. *Unified growth theory*; Princeton University Press, 2011.
47. Caselli, F.; Coleman, W.J. The U.S. structural transformation and regional convergence: A reinterpretation. *Journal of political Economy* **2001**, *109*, 584–616.
48. Gollin, D.; Lagakos, D.; Waugh, M.E. The Agricultural Productivity Gap. *Quarterly Journal of Economics* **2014**, *129*, 939–993.
49. Kennan, J.; Walker, J.R. The Effect of Expected Income on Individual Migration Decisions. *Econometrica* **2011**, *79*, 211–251. doi:10.3982/ECTA4657.
50. di Giovanni, J.; Levchenko, A.A.; Ortega, F. A Global View of Cross-Border Migration. *Journal of the European Economic Association* **2015**, *13*, 168–202. doi:10.1111/jeea.12110.
51. Desmet, K.; Rossi-Hansberg, E. On the spatial economic impact of global warming. *Journal of Urban Economics* **2015**, *88*, 16–37.
52. Solt, F. The Standardized World Income Inequality Database*. *Social Science Quarterly* **2016**, *97*, 1267–1281. doi:10.1111/ssqu.12295.
53. Zilberman, D.; Liu, X.; Roland-Holst, D.; Sunding, D. The economics of climate change in agriculture. *Mitigation and Adaptation Strategies for Global Change* **2004**, *9*, 365–382.
54. Nelson, G.C.; Van Der Mensbrugghe, D.; Ahammad, H.; Blanc, E.; Calvin, K.; Hasegawa, T.; Havlik, P.; Heyhoe, E.; Kyle, P.; Lotze-Campen, H.; et al. Agriculture and climate change in global scenarios: why don't the models agree. *Agricultural Economics* **2014**, *45*, 85–101.
55. Lutz, W.; Butz, W.P.; Samir, K. *World population and human capital in the twenty-first century*; OUP Oxford, 2014.
56. Lutz, W.; Butz, W.P.; Samir, K. *World population & human capital in the twenty-first century: An overview*; Oxford University Press, 2017.
57. Dotti Sani, G.M.; Treas, J. Educational Gradients in Parents' Child-Care Time Across Countries, 1965–2012. *Journal of Marriage and Family* **2016**, *78*, 1083–1096.
58. O'Neill, B.C.; Kriegler, E.; Ebi, K.L.; Kemp-Benedict, E.; Riahi, K.; Rothman, D.S.; van Ruijven, B.J.; van Vuuren, D.P.; Birkmann, J.; Kok, K.; et al. The roads ahead: Narratives for shared socioeconomic pathways describing world futures in the 21st century. *Global Environmental Change* **2017**, *42*, 169–180. doi:10.1016/j.gloenvcha.2015.01.004.
59. Suckall, N.; Fraser, E.; Forster, P. Reduced migration under climate change: evidence from Malawi using an aspirations and capabilities framework. *Climate and Development* **2017**, *9*, 298–312.
60. Adger, W.N.; Arnell, N.W.; Black, R.; Dercon, S.; Geddes, A.; Thomas, D.S. Focus on environmental risks and migration: causes and consequences. *Environmental Research Letters* **2015**, *10*, 060201.